
THE
EMBO
JOURNAL
Volume 34 Issue 24 | 14 December 2015
CISPLATIN
CHLORIDE
TAURINE
H2O
VRAC channels
osmolytes and cancer drugs
COVER IMAGE © T.J. JENTSCH & R. PLANELLS-CASES
FMP/MDC BERLIN | GERMANY
EMBOpress

Published online: November 3, 2015

Article

TRANSPARENT PROCESS OPEN ACCESS

THE EMBO JOURNAL

Subunit composition of VRAC channels determines substrate specificity and cellular resistance to Pt-based anti-cancer drugs

Rosa Planells-Cases[1], Darius Lutter[1], Charlotte Guyader[2], Nora M Gerhards[3], Florian Ullrich[1], Deborah A Elger[1], Asli Kucukosmanoglu[4], Guotai Xu[4], Felizia K Voss[1], S Momsen Reincke[1], Tobias Stauber[1,†], Vincent A Blomen[5], Daniel J Vis[6], Lodewyk F Wessels[6], Thijn R Brummelkamp[5], Piet Borst[2], Sven Rottenberg[3,4,*] & Thomas J Jentsch[1,7,**]

Abstract

Although platinum-based drugs are widely used chemotherapeutics for cancer treatment, the determinants of tumor cell responsiveness remain poorly understood. We show that the loss of subunits LRRC8A and LRRC8D of the heteromeric LRRC8 volume-regulated anion channels (VRACs) increased resistance to clinically relevant cisplatin/carboplatin concentrations. Under isotonic conditions, about 50% of cisplatin uptake depended on LRRC8A and LRRC8D, but neither on LRRC8C nor on LRRC8E. Cell swelling strongly enhanced LRRC8-dependent cisplatin uptake, bolstering the notion that cisplatin enters cells through VRAC. *LRRC8A* disruption also suppressed drug-induced apoptosis independently from drug uptake, possibly by impairing VRAC-dependent apoptotic cell volume decrease. Hence, by mediating cisplatin uptake and facilitating apoptosis, VRAC plays a dual role in the cellular drug response. Incorporation of the LRRC8D subunit into VRAC substantially increased its permeability for cisplatin and the cellular osmolyte taurine, indicating that LRRC8 proteins form the channel pore. Our work suggests that LRRC8D-containing VRACs are crucial for cell volume regulation by an important organic osmolyte and may influence cisplatin/carboplatin responsiveness of tumors.

Keywords chloride channel; haploid cell screen; swelling-activated; VSOAC; VSOR

Subject Categories Autophagy & Cell Death; Cancer; Membrane & Intracellular Transport

DOI 10.15252/embj.201592409 | Received 30 June 2015 | Revised 4 October 2015 | Accepted 5 October 2015 | Published online 3 November 2015

The EMBO Journal (2015) 34: 2993–3008

See also: **T Voets *et al*** (December 2015)

Introduction

The platinum-containing drugs cisplatin, carboplatin, and oxaliplatin are among the most successful drugs used for treating cancer (Kelland, 2007). Pt drugs introduce covalent adducts in DNA which eventually cause cell death. Tumor cells treated with therapeutic doses of Pt drugs probably die predominantly by mitotic catastrophe/necrosis (Borst *et al*, 2001; Brown & Attardi, 2005). Attempts to link Pt drug sensitivity to apoptosis remain prominent (Speirs *et al*, 2011), however, even though the induction of apoptosis by high drug concentrations has been shown to be due to a cytoplasmic off-target effect of Pt drugs (Mandic *et al*, 2003; Berndtsson *et al*, 2007; Fayad *et al*, 2009).

In cultured cells, the induction of apoptosis by cisplatin and other drugs such as staurosporine is characterized by an early cell shrinkage denominated apoptotic volume decrease (AVD) which is followed by other apoptotic hallmarks like the activation of caspases and DNA fragmentation. AVD and the induction of apoptosis could be inhibited by blockers of the ubiquitously expressed volume-regulated anion channel VRAC (also known as VSOR or VSOAC) (Maeno *et al*, 2000; Ise *et al*, 2005; Okada *et al*, 2006; Lang & Hoffmann, 2012). Being closed under resting conditions, VRAC opens upon cell swelling and releases chloride and organic osmolytes in the course of regulatory volume decrease (RVD). The effect of VRAC blockers on drug-induced apoptosis was attributed to a loss of VRAC-dependent AVD (Maeno *et al*, 2000). However, the blockers used to substantiate a role of VRAC in apoptosis are all non-specific, and the notion that AVD facilitates apoptosis is controversial (Orlov *et al*, 2013). VRAC has been characterized biophysically and physiologically for decades, but the failure to identify the underlying proteins (Okada, 1997; Pedersen *et al*, 2015)

1 Leibniz-Institut für Molekulare Pharmakologie (FMP), Max-Delbrück-Centrum für Molekulare Medizin (MDC), Berlin, Germany
2 Division of Molecular Oncology, The Netherlands Cancer Institute, Amsterdam, The Netherlands
3 Institute of Animal Pathology, Vetsuisse Faculty, University of Bern, Bern, Switzerland
4 Division of Molecular Pathology, The Netherlands Cancer Institute, Amsterdam, The Netherlands
5 Division of Biochemistry, The Netherlands Cancer Institute, Amsterdam, The Netherlands
6 Division of Molecular Carcinogenesis, The Netherlands Cancer Institute, Amsterdam, The Netherlands
7 NeuroCure Cluster of Excellence, Charité Universitätsmedizin, Berlin, Germany
*Corresponding author. Tel: +41 31 6312395; E-mail: sven.rottenberg@vetsuisse.unibe.ch
**Corresponding author. Tel: +49 30 94062961; E-mail: Jentsch@fmp-berlin.de
†Present address: Institute of Chemistry and Biochemistry, Freie Universitaet Berlin, Berlin

precluded conclusive genetic and biochemical studies. Only recently, LRRC8 heteromers were identified as essential VRAC components. LRRC8A is an obligatory VRAC subunit (Qiu *et al*, 2014; Voss *et al*, 2014), but it needs at least one other LRRC8 homolog (LRRC8B, LRRC8C, LRRC8D, or LRRC8E) to mediate volume-activated anion currents ($I_{Cl,vol}$) or to release organic osmolytes like taurine (Voss *et al*, 2014). A weak homology to pannexins suggests that LRRC8 proteins may assemble to hexameric channels (Abascal & Zardoya, 2012). The formation of different LRRC8 heteromers indicates that there are several different VRACs that may vary in properties and tissue distribution. For instance, the subunit composition of LRRC8 heteromers might specify the channel's preference for chloride over taurine or vice versa. Such a scenario would support the contentious notion (Lambert & Hoffmann, 1994; Stutzin *et al*, 1999; Shennan, 2008) that VRAC is molecularly distinct from a postulated volume-stimulated organic osmolyte/anion channel VSOAC (Jackson & Strange, 1993). However, the impact of specific LRRC8 subunits on VRAC's selectivity has not yet been investigated.

An unbiased genomic screen now revealed that the loss of either of two VRAC subunits, LRRC8A or LRRC8D, increased resistance against carboplatin and cisplatin. This finding can be largely explained by an unsuspected role of VRAC in drug transport. This transport required the obligatory channel subunit LRRC8A and also depended on LRRC8D, a subunit that strongly increased VRAC's permeability to cisplatin/carboplatin. Exposure to staurosporine revealed an additional, drug uptake-independent, but possibly AVD-related effect of LRRC8A on drug-induced apoptosis. Moreover, LRRC8D increased VRAC's permeability to taurine, and cells lacking this subunit showed reduced cell volume regulation. Our work uncovers a novel role of VRAC in cisplatin and carboplatin uptake and resistance, identifies LRRC8A/LRRC8D-containing VRACs as physiologically important organic osmolyte channels, and reveals differences in substrate selectivity and pharmacology between differently composed VRACs.

Results

A genomewide screen identifies LRRC8A and LRRC8D as mediators of carboplatin and cisplatin resistance

To identify genes affecting platinum drug sensitivity, we performed genomewide loss-of-function screens of haploid KBM7 cells that were subjected to insertional mutagenesis using a gene-trap virus (Carette *et al*, 2009) (Fig 1A). Cells resisting exposure to 7 μM carboplatin for three weeks showed a significant enrichment of insertions in the *LRRC8D* and *LRRC8A* genes (Fig 1B and Appendix Table S1). Most sense insertions were localized in introns upstream of the ORF-containing exon 3 (Fig 1C). These positions are consistent with gene-inactivating mutations. Two *LRRC8D*-deficient KBM7 clones, which display reduced blasticidin S uptake (Lee *et al*, 2014) and which lack the LRRC8D protein (Fig EV1), were indeed more resistant to both carboplatin and cisplatin, but not to the larger compound oxaliplatin (Fig 1D and Appendix Table S2). Likewise, KBM7-derived haploid HAP1 cells (Carette *et al*, 2011) were resistant to carboplatin and cisplatin, but not to oxaliplatin, when *LRRC8A* or *LRRC8D* was disrupted (Fig EV2). Hence, two genes, *LRRC8A* and *LRRC8D*, affected carbo- and cisplatin sensitivity at drug concentrations that can be achieved in patients.

Low *LRRC8D* expression correlates with reduced survival of Pt drug-treated ovarian cancer patients

To determine whether *LRRC8A* or *LRRC8D* expression might affect chemotherapy in patients, we examined The Cancer Genome Atlas (TCGA) data collection of ovarian cancer patients who were treated with platinum drugs. We analyzed the survival of patients with a low tumor expression of *LRRC8A* or *LRRC8D* versus the remaining patients. We used the lower tertile of the distribution of *LRRC8A* and *LRRC8D* expressions as cutoff. Whereas low *LRRC8A* expression had no influence on survival (Fig 2A), patients with a low *LRRC8D* gene expression in their ovarian cancers displayed a significantly reduced survival (Fig 2B). Most patients had also received taxane, but disruption of *LRRC8A* or *LRRC8D* did not provide resistance against docetaxel (Appendix Fig S1). To corroborate these results, we investigated the data derived from ovarian cancer patients that were recently published by Patch *et al* (2015). Although the available data are derived from fewer patients, also in this analysis a low expression of *LRRC8D,* but not *LRRC8A*, correlated with a modest, but significant decrease in survival (Fig 2C and D). Thus, *LRRC8D* might also affect platinum drug responses in cancer patients.

Pt drug resistance is not strictly correlated with lack of VRAC currents or volume regulation

LRRC8A and LRRC8D are subunits of the volume-regulated anion channel VRAC. The finding that the loss of LRRC8D conferred drug resistance was surprising because this subunit, unlike LRRC8A, is dispensable for VRAC Cl^- currents ($I_{Cl,vol}$) in HCT116 cells (Voss *et al*, 2014), a finding we now confirmed for haploid HAP1 and KBM7 cells (Fig 3A and B, Appendix Fig S2). Hence, Pt drug resistance is not correlated with a loss of VRAC Cl^- channel activity.

In view of the postulated role of VRAC activation in cisplatin-induced cell shrinkage and subsequent apoptotic cell death (Maeno *et al*, 2000; Okada *et al*, 2006; Lang & Hoffmann, 2012), we explored the role of LRRC8A and LRRC8D in regulatory volume decrease (RVD) that can be determined more reliably than AVD. Like $I_{Cl,vol}$ (Voss *et al*, 2014), RVD depended on LRRC8 heteromers because it was similarly impaired in $LRRC8A^{-/-}$ and $LRRC8(B,C,D,E)^{-/-}$ cells that lack LRRC8 isoforms B through E (Fig 3C). In $LRRC8D^{-/-}$ cells, notwithstanding unchanged $I_{Cl,vol}$ amplitudes (Fig 3A and B; Voss *et al*, 2014), RVD was significantly reduced but not abolished (Fig 3C). Hence, it seems unlikely that *LRRC8D* disruption protects cells against cisplatin toxicity by impairing VRAC- and AVD-dependent apoptosis.

LRRC8-dependent induction of apoptosis by cisplatin and staurosporine

We next measured drug-induced activation of caspase-3 to test whether the induction of apoptosis by staurosporine or high concentrations of cisplatin depends on LRRC8 subunits. Cisplatin-induced caspase activation was indeed suppressed in $LRRC8A^{-/-}$,

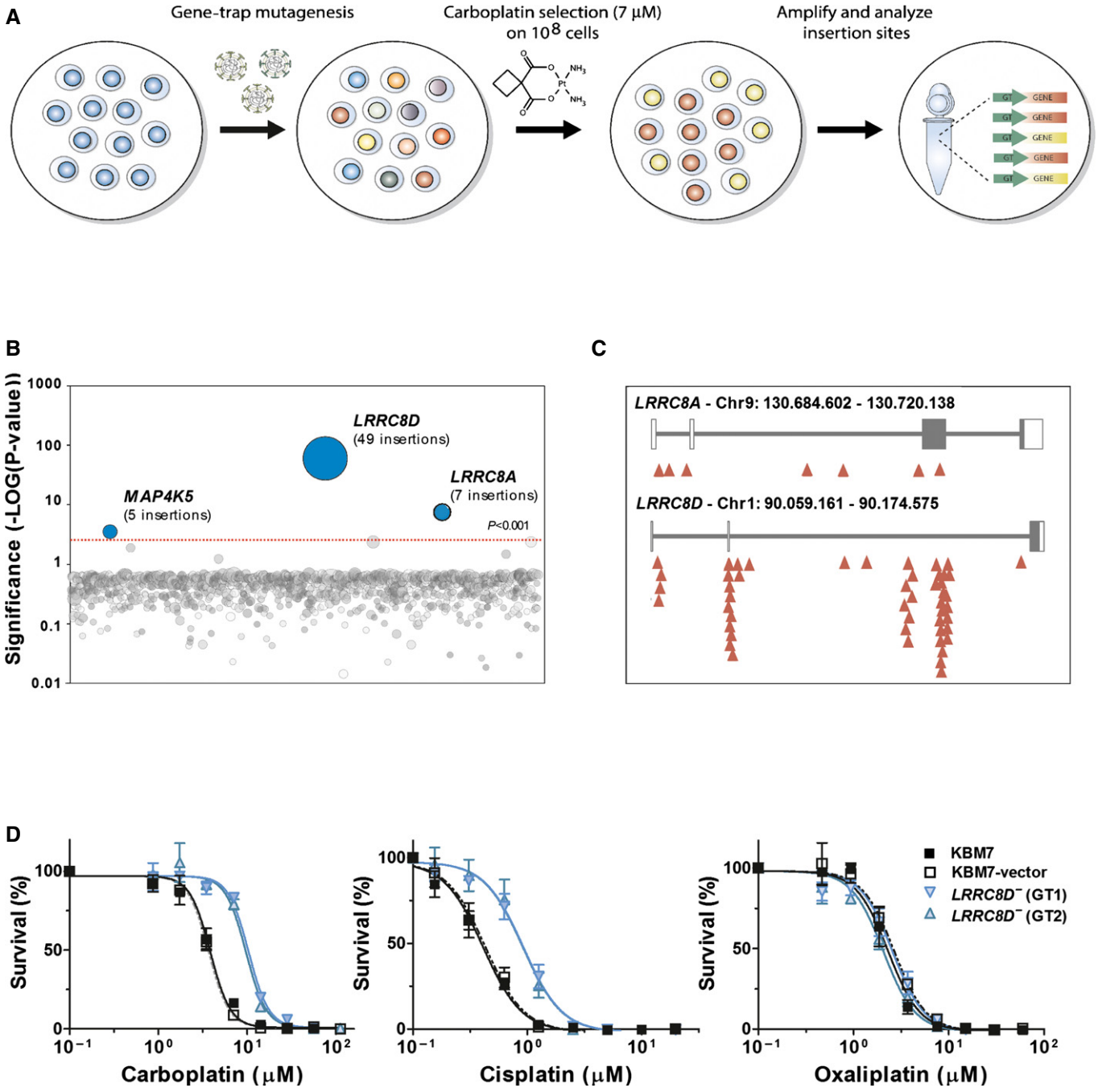

Figure 1. Loss-of-function screen using haploid KBM7 cells identifies LRCC8A and LRRC8D as determinants of carboplatin resistance.

A Outline of the loss-of-function screen.

B Genes enriched for gene-trap insertions in a carboplatin-selected cell population compared to unselected control cells. Circles represent genes and their size corresponds to the number of independent insertions identified in the carboplatin-selected population. Genes are ranked on the *x*-axis based on chromosomal position.

C Location of gene-trap insertion sites (red arrowheads). White boxes indicate the 5′- and 3′-untranslated regions, and the black boxes show the coding sequence in exons 3 and 4 (*LRRC8A*) and exon 3 (*LRRC8D*).

D Loss of LRRC8D causes resistance to carboplatin and cisplatin, but not to oxaliplatin. Survival of parental, vector-transduced, or LRRC8D-deficient GT1 and GT2 KBM7 cells exposed for 96 h to increasing concentrations of cisplatin, carboplatin, and oxaliplatin. The corresponding IC_{50} values and 95% confidence interval (CI) are given in Appendix Table S2. Data are presented as mean ± SEM.

LRRC8D$^{-/-}$, and *LRRC8*$^{-/-}$ cells that lack all LRRC8 subunits (Fig 4A). To explore whether activation of VRAC by hypotonic swelling facilitated cisplatin-induced apoptosis, we exposed cells during 1 h to 200 μM cisplatin in hypotonic medium (−25%) and measured caspase activity after 1 to 3 days. This procedure drastically increased caspase activation in WT cells (Fig 4B).

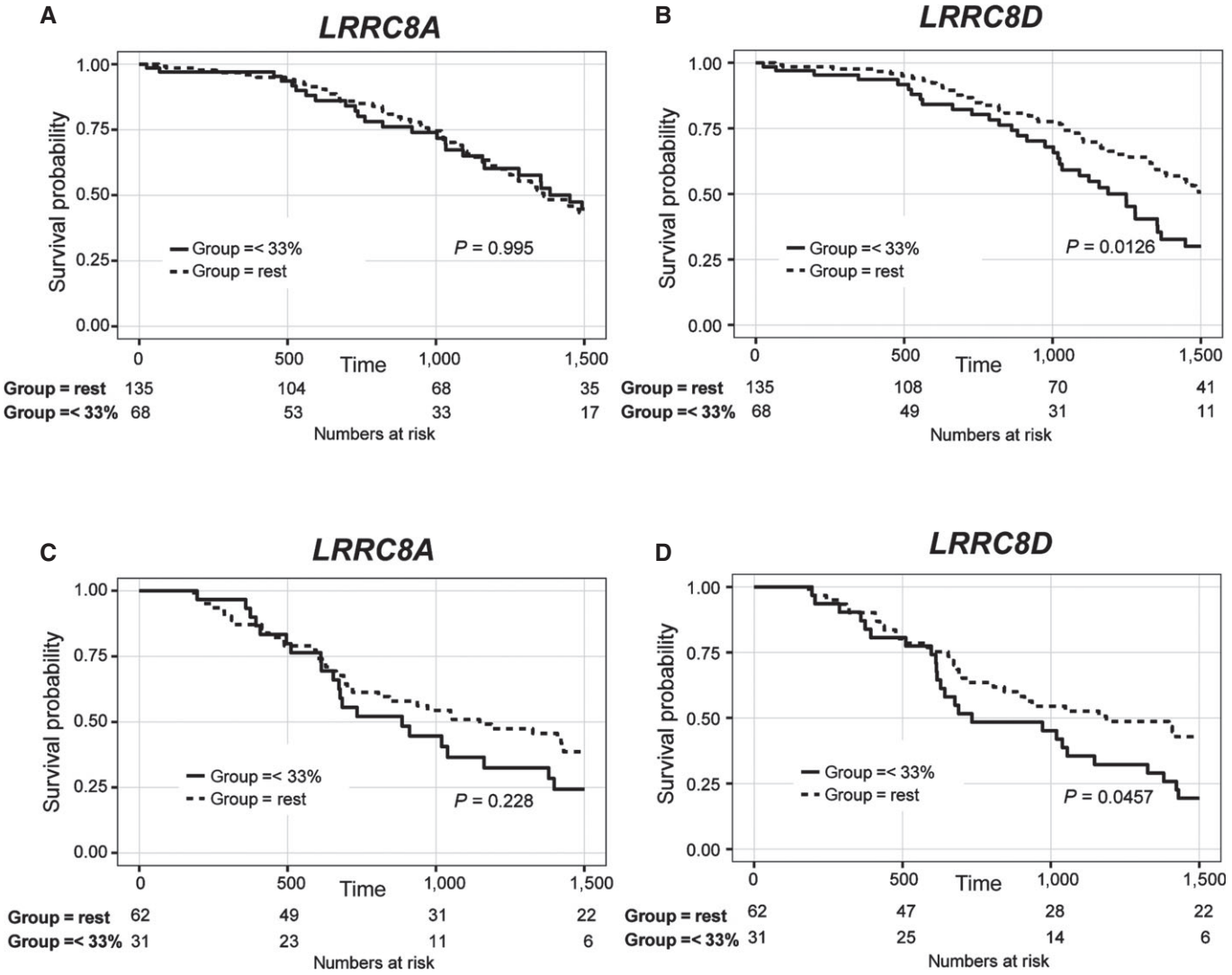

Figure 2. Low expression of *LRRC8D* but not *LRRC8A* correlates with shorter survival of high grade serous ovarian cancer patients treated with platinum-based drugs.

A–D Differential survival based on *LRRC8A* (A, C) or *LRRC8D* (B, D) gene expression as extracted from the TCGA database (http://cancergenome.nih.gov/) (A, B) or using the data from Patch *et al* (2015) (C, D). As cutoff the lower tertile of LRRC8A or LRRC8D gene expression was used. *P*-values were determined using the log-rank test.

Swelling-enhanced caspase induction by cisplatin depended on VRAC as it was abolished in *LRRC8A*$^{-/-}$ and *LRRC8*$^{-/-}$ cells. It was strongly reduced, but not abolished, in *LRRC8D*$^{-/-}$ cells (Fig 4B).

By contrast, staurosporine-induced caspase activation was not enhanced by hypotonic swelling and was suppressed in *LRRC8A*$^{-/-}$, but not in *LRRC8D*$^{-/-}$ cells (where it was rather increased for unknown reasons) (Fig 4C). Since both $I_{Cl,vol}$ and caspase induction by staurosporine depend on LRRC8A but not LRRC8D, these results are compatible with the hypothesis that VRAC activation-dependent AVD facilitates the progression of apoptosis (Maeno *et al*, 2000; Shimizu *et al*, 2004). VRAC activation by pro-apoptotic stimuli was monitored by the quenching of YFP fluorescence by externally added iodide (Voss *et al*, 2014). Iodide permeates VRAC efficiently and hence VRAC opening increases YFP quenching rates. The slow emergence of an LRRC8A-dependent quenching component upon incubation with 200 μM cisplatin (Fig 5A–C) or 4 μM staurosporine indicated that both drugs slowly activated VRAC (Fig 5E and F). Drug-induced VRAC activation was small compared to that elicited by acute hypotonic cell swelling (Fig 5D). A direct comparison of quenching slopes, however, underestimates the difference in activation because quenching rates after acute exposure to hypotonicity (but not with drug preincubation) also reflect the time course of cell swelling and ensuing VRAC opening (Appendix Fig S2A and E).

VRAC mediates cisplatin uptake which depends on LRRC8 subunit composition

The observation that cisplatin activated caspase-3 in WT cells more efficiently when applied in hypotonic medium suggested that cisplatin might enter cells through VRACs. Indeed, VRACs not only conduct halide ions, but also organic compounds like taurine,

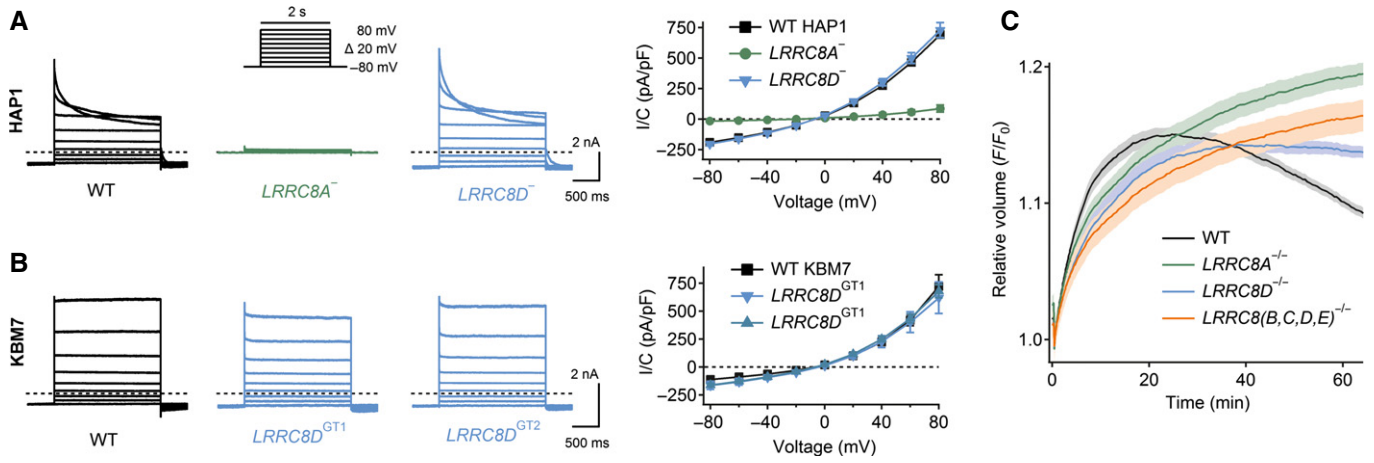

Figure 3. Disruption of *LRRC8A*, but not of *LRRC8D*, abolishes $I_{Cl,vol}$ and blocks volume regulation.

A, B VRAC currents ($I_{Cl,vol}$) of the HAP1 (A) and KBM7 (B) haploid cell lines. Left panels, example current traces of $I_{Cl,vol}$ fully activated by hypotonic cell swelling measured with the voltage-clamp protocol shown in (A). Dashed lines indicate zero current. Right panels, averaged current/voltage relationships of maximally activated $I_{Cl,vol}$. Consistent with VRAC currents, they needed hypotonic swelling for activation, displayed an $I^- > Cl^-$ permeability sequence, and were blocked by DCPIB (Appendix Fig S2A–H). The difference in current inactivation between HAP1 and KBM7 cells can be explained by the fact that KBM7 cells hardly express LRRC8E (Fig EV1) which accelerates VRAC inactivation (Voss *et al*, 2014). At potentials > +100 mV, also KBM7 currents inactivated (Appendix Fig S2I). Data are presented as mean ± SEM; n = 5–10.

C Dependence of regulatory volume decrease (RVD) of HEK cells on *LRRC8* genes. Cells were exposed to hypotonic medium starting at t = 0, and intracellular calcein fluorescence was followed over ~1 h as semiquantitative measure of cell volume. Data are presented as mean values ± SEM from sixteen wells.

glutamate, and blasticidin (Jackson & Strange, 1993; Hyzinski-García *et al*, 2014; Lee *et al*, 2014; Qiu *et al*, 2014; Voss *et al*, 2014). Importantly, early studies on a variety of cultured cell lines have led to the conclusion that cisplatin/carboplatin uptake involves two components: About half the drug enters cells by passive diffusion through the plasma membrane and the other half via a protein component, possibly a channel (reviewed by Gately & Howell, 1993). We therefore measured the cellular accumulation of Pt-based drugs by determining Pt concentrations in extracts of cells of various LRRC8 genotypes.

Under isotonic conditions, drug uptake performed at therapeutic carboplatin concentrations (7 μM) by drug-resistant *LRRC8D*$^{-/-}$ KBM7 cell clones was indeed reduced ~twofold compared to control (Fig 6A). The effect of VRAC subunits in Pt drug uptake was explored in detail for cisplatin in HEK and HCT116 cells of different *LRRC8* genotypes. The underlying uptake processes did not saturate with cisplatin concentrations up to 400 μM in both WT and *LRRC8A*$^{-/-}$ cells (Fig EV3), allowing us to use concentrations exceeding therapeutic levels to increase the sensitivity of the assay. When uptake was performed over several hours under isotonic conditions, cisplatin accumulation was reduced by roughly 70 and 50% upon disruption of *LRRC8A* or *LRRC8D*, respectively (Fig 6C (HEK cells), Fig EV4A (HCT cells)). This subunit dependence resembled that observed with cellular carboplatin and cisplatin resistance (Figs 1 and EV2). The LRRC8-dependent uptake component increased with variable time course over the first few hours (Figs 6C and E, EV4A and EV5). When uptake was studied in isotonic saline for 1 h or less, no significant influence of either LRRC8A or LRRC8D was detected (Fig 6D and E, highlighted by dashed line, and Fig EV4B). Isotonic cisplatin uptake thus appears to be associated with a rather slow activation of VRAC in these cells, which we (Fig 5) and others (Shimizu *et al*, 2004; Poulsen *et al*, 2010; Min *et al*, 2011; Cai *et al*, 2015) have observed in response to pro-apoptotic drugs.

Hypotonic cell swelling activates VRAC anion currents within a few minutes (Nilius *et al*, 1997; Voss *et al*, 2014) (Appendix Fig S2A and E). A 25% decrease in osmolarity during 15- or 60-min uptake periods indeed increased cisplatin accumulation several-fold (Figs 6D and F (HEK), and EV4B, Appendix Fig S3 (HCT116)). Whereas long-term isotonic uptake was almost as strongly reduced in *LRRC8D*$^{-/-}$ as in *LRRC8A*$^{-/-}$ cells, the hypotonicity-stimulated cisplatin uptake component was abolished in *LRRC8A*$^{-/-}$ cells, but reduced by only up to 50% in *LRRC8D*$^{-/-}$ cells (Figs 6D (HEK) and EV4B (HCT116)). Like $I_{Cl,vol}$ (Voss *et al*, 2014), swelling-induced cisplatin uptake was normal in *LRRC8C*$^{-/-}$ cells (Fig 6D), abolished in *LRRC8(B,C,D,E)*$^{-/-}$ cells (which express only LRRC8A) (Appendix Fig S3), and was suppressed by the VRAC inhibitor carbenoxolone (Ye *et al*, 2009; Voss *et al*, 2014) (Fig 6B). These findings indicated that VRACs (LRRC8 heteromers) transport Pt-based drugs and suggest a special role of LRRC8D-containing channels.

VRACs might be hetero-hexamers of LRRC8 proteins (Abascal & Zardoya, 2012; Voss *et al*, 2014), and HEK and HCT116 cells express all five *LRRC8* genes (Fig EV1). This suggests a highly heterogeneous VRAC population. We reduced this complexity by studying *LRRC8(B,D,E)*$^{-/-}$, *LRRC8(B,C,E)*$^{-/-}$, and *LRRC8(B,C,D)*$^{-/-}$ cells that can only express LRRC8A/C, LRRC8A/D, and LRRC8A/E heteromeric channels, respectively. Long-term, isotonic cisplatin accumulation by A/D-expressing cells was much larger than by *LRRC8A*$^{-/-}$ cells (Figs 6E and EV5), whereas cells expressing A/C heteromers (Fig 6E) or A/E heteromers (Fig EV5) took up as little cisplatin as *LRRC8A*$^{-/-}$ cells. Hypotonicity enhanced short-term cisplatin uptake to almost the same extent in WT- and LRRC8A/D-expressing cells (Fig 6F). LRRC8A/C heteromers appeared to enable cisplatin uptake upon cell swelling, but to a

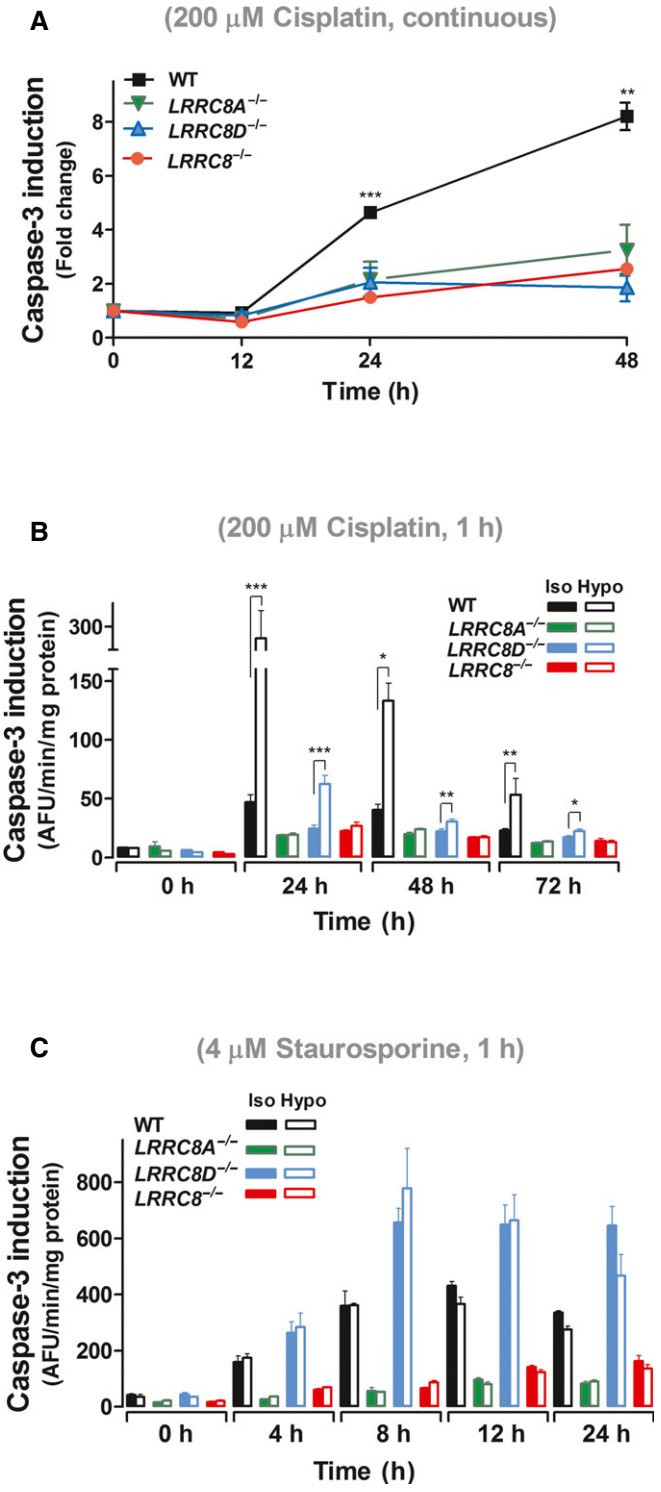

Figure 4. LRRC8 subunit- and osmolarity-dependent caspase induction in HCT116 cells.

A, B Cisplatin-induced caspase activity in the continuous presence of 200 μM cisplatin under isotonic conditions (A), or after 1 h exposure to 200 μM cisplatin under iso- and hypotonic conditions (B), was followed over time in WT, *LRRC8A*$^{-/-}$, *LRRC8D*$^{-/-}$, and *LRRC8*$^{-/-}$ HCT116 cells. Results from *LRRC8A*$^{-/-}$ and *LRRC8D*$^{-/-}$ were obtained with two different clonal cell lines each and averaged.

C Caspase activation after 1-h exposure to 4 μM staurosporine under iso- or hypotonic conditions of WT, *LRRC8A*$^{-/-}$, *LRRC8D*$^{-/-}$, and *LRRC8*$^{-/-}$ HCT116 cells.

Data information: Data are presented as mean ± SEM, $n = 3$–6. *$P < 0.05$; **$P < 0.01$; and ***$P < 0.001$. Similar results were obtained in three independent experiments. Fold change in (A) refers to $t = 0$. Control experiments indicated that hypotonicity *per se* had no effect (Appendix Fig S4).

much smaller degree than LRRC8A/D heteromers or WT VRAC (Fig 6F). Importantly, amplitudes of swelling-activated Cl^- currents of A/C-expressing cells were similar to WT $I_{Cl,vol}$, but were much smaller with A/D heteromers (Fig 6G)—a finding agreeing with heterologous expression studies (Voss *et al*, 2014). Hence, LRRC8D-containing heteromers display a considerably higher cisplatin/Cl^- transport ratio than other LRRC8 heteromers (Fig 6H).

VRAC Cl^- currents are inhibited by cisplatin–DMSO complexes in a LRRC8D-dependent manner

In a high-throughput drug screen for VRAC transport inhibitors, in which compounds were routinely dissolved in DMSO, we identified cisplatin as putative VRAC blocker (*data not shown*). However, suppression of $I_{Cl,vol}$ required DMSO, with which cisplatin forms adducts like $Pt(NH_3)_2(Cl)(DMSO)$ (Fischer *et al*, 2008). Cisplatin–DMSO complexes inhibited native $I_{Cl,vol}$ of HEK cells in a dose-dependent manner (Fig 7A), but had no effect on currents of *LRRC8D*$^{-/-}$ cells (Fig 7B). Hence, differently composed LRRC8 channels can also differ in their pharmacology, and cisplatin-conducting VRACs might be specifically targeted without abolishing $I_{Cl,vol}$ and cell volume regulation.

Swelling-induced release of the cellular osmolyte taurine depends on LRRC8D

Whereas *LRRC8D*$^{-/-}$ cells displayed unchanged swelling-activated Cl^- currents ($I_{Cl,vol}$) (Figs 3A and B, and 6G; Voss *et al*, 2014), their RVD was markedly decreased (Fig 3C). We therefore hypothesized that LRRC8D is not only important for the transport of cis- and carboplatin, but also of organic osmolytes that do not contribute to electric currents. Indeed, *LRRC8D* disruption drastically reduced swelling-induced efflux of the important cellular osmolyte taurine (Fig 8A), but had less of an effect than disruption of *LRRC8A* that apparently totally abolishes swelling-induced taurine efflux (Voss *et al*, 2014). Transient transfection of *LRRC8D*, which is difficult to express heterologously (Voss *et al*, 2014), partially rescued taurine efflux (Fig 8B). Taurine efflux from A/D-expressing cells resembled WT fluxes (Fig 8C), whereas LRRC8C or LRRC8E failed to support significant taurine flux as revealed by experiments with *LRRC8(B,D,E)*$^{-/-}$ and *LRRC8(B,C,D)*$^{-/-}$ cells in which only LRRC8A and LRRC8C or LRRC8E, respectively, remain (Fig 8D and E). The reduced RVD of *LRRC8D*$^{-/-}$ cells (Fig 3C) thus exposes the importance of taurine and possibly other organic osmolytes in cell volume regulation.

Like VRAC-dependent I^- influx (Fig 5A–C), also VRAC-mediated taurine efflux was stimulated by preincubation with cisplatin (Fig 8F). In congruence with the weaker stimulation of iodide flux by cisplatin than by hypotonicity (Fig 3), cisplatin preincubation stimulated taurine efflux much less than hypotonic swelling. The cisplatin-induced efflux component increased with the time of

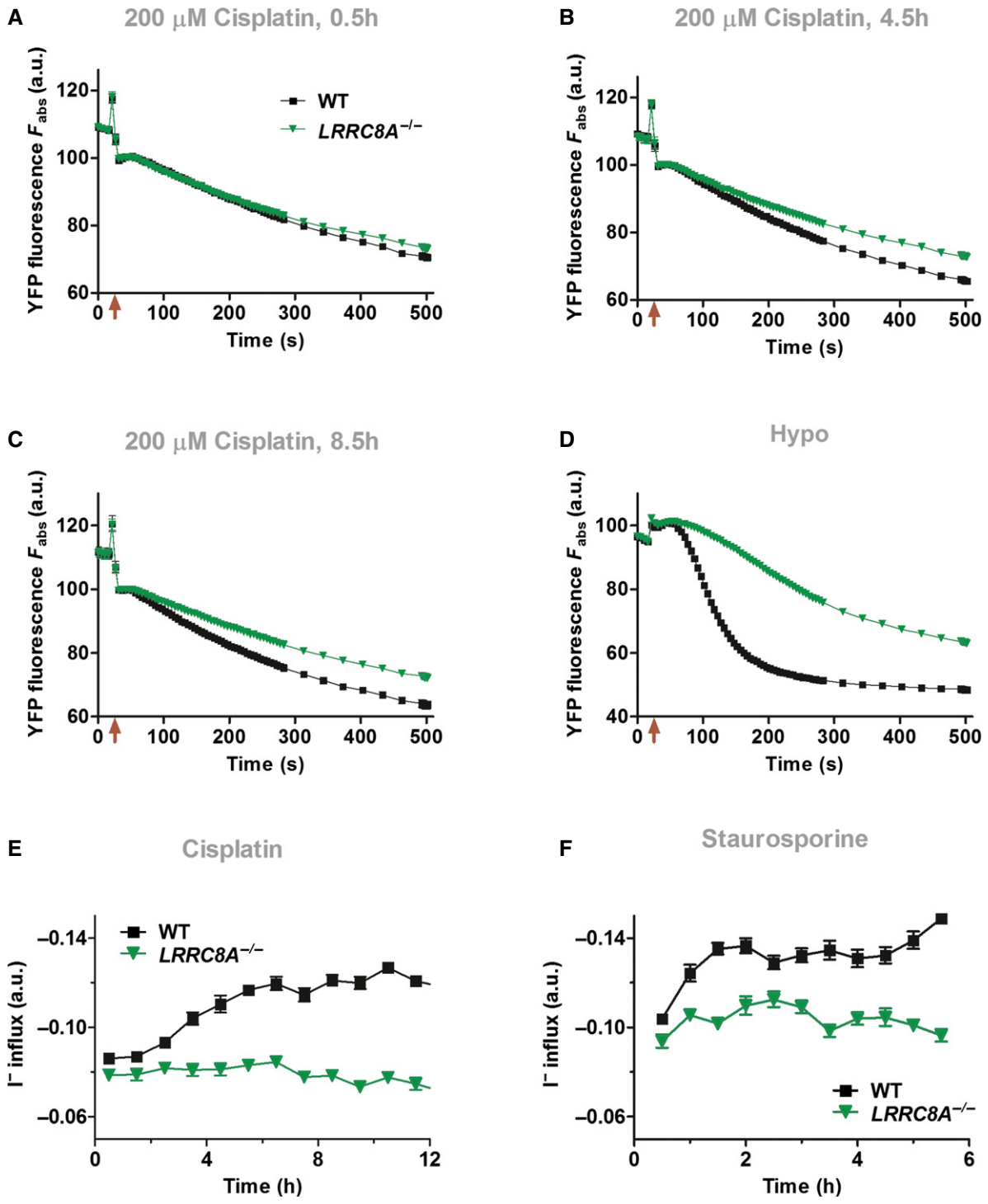

Figure 5. Activation of LRRC8 channels by pro-apoptotic stimuli.

A–C Cisplatin-induced iodide influx into WT (black ■), but not *LRRC8A*$^{-/-}$ (green ▼) HEK cells indicates VRAC halide current activation during apoptosis. Cells expressing an iodide-sensitive YFP variant were exposed to 200 μM cisplatin for periods of 0.5 h (A), 4.5 h (B), or 8.5 h (C) before adding extracellular I^- (50 mM final). The difference in slopes of YFP fluorescence quenching between control and cisplatin-treated cells semiquantitatively reflects VRAC current activation. Note that increased YFP quenching with cisplatin preincubation is not due to large non-specific leaks resulting from cell morbidity. Such leaks should lead to a fast component of YFP quenching in WT, but not *LRRC8A*$^{-/-}$ cells after the pipetting artifact that immediately follows addition of iodide (indicated by arrows).

D Swelling-induced iodide influx into WT (black ■) and *LRRC8A*$^{-/-}$ (green ▼) HEK cells for comparison. Iodide (50 mM final) was added in isotonic or hypotonic (230 mOsm final) solution at the time indicated by arrow.

E, F Time course of VRAC activation by 200 μM cisplatin (E) or 4 μM staurosporine (F) determined as in (A–C). Averaged maximal slopes of YFP quenching from eight wells (E) or 16 wells (F) each were evaluated to estimate iodide influx rates. WT (black ■) and *LRRC8A*$^{-/-}$ (green ▼). Data are presented as mean ± SEM.

preincubation and was abolished in *LRRC8A*$^{-/-}$ cells. Taurine efflux did not occur through cell morbidity-related unspecific leaks since it could be blocked by carbenoxolone (Fig. 8F). WT VRACs seemed to transport taurine at low rates also without stimulation by cisplatin as indicated by the reduced efflux from cells lacking LRRC8A. However, at these low transport rates, we cannot exclude that slight and variable osmotic imbalances marginally opened VRAC as steady-state efflux differed between experiments (compare Fig 8A–E).

Discussion

Our work indicates that heteromeric LRRC8 channels (VRACs) can transport cisplatin and carboplatin, widely used anti-cancer drugs, and that the substrate selectivity and pharmacology of VRAC depend on its subunit composition. LRRC8D plays important pharmacological and physiological roles in supporting the transport of anti-cancer drugs and of the organic osmolyte taurine. LRRC8 channels also facilitated drug-induced apoptosis independent of drug transport, revealing a dual role of VRAC in cisplatin toxicity.

LRRC8 channels in drug-induced apoptosis

Several groups have reported that inhibition of *bona fide* VRAC (VSOR, VSOAC) by various non-specific compounds impaired the induction of apoptosis by drugs such as cisplatin and staurosporine (Maeno *et al*, 2000; Ise *et al*, 2005; Okada *et al*, 2006; d'Anglemont de Tassigny *et al*, 2008; Poulsen *et al*, 2010). These findings were attributed to an impairment of VRAC-dependent apoptotic volume decrease (AVD) which is thought to be crucial for the progression of apoptosis (Maeno *et al*, 2000) (for recent reviews, see Hoffmann & Lambert, 2014; Lang & Hoffmann, 2012). Indeed, cisplatin and other drugs lead to a slow activation of currents with typical characteristics of $I_{Cl,vol}$, and the resulting AVD could be reduced by non-specific VRAC inhibitors (Shimizu *et al*, 2004; Poulsen *et al*, 2010; Min *et al*, 2011; Cai *et al*, 2015). Moreover, several cancer drug-resistant cell lines display less $I_{Cl,vol}$, AVD, RVD, and swelling-activated taurine efflux than their parent cells (Lee *et al*, 2007; Poulsen *et al*, 2010; Min *et al*, 2011; Sørensen *et al*, 2014). In KCP-4 cells, both cisplatin sensitivity and $I_{Cl,vol}$ were partially restored in parallel by non-specific changes in gene expression using a histone deacetylase inhibitor (Lee *et al*, 2007). Since some of those cell lines are resistant to various anti-cancer drugs that probably enter cells through different pathways, these reports suggested that VRAC downregulation entailed drug resistance through an AVD-dependent mechanism.

Because LRRC8A was required for both $I_{Cl,vol}$ and pro-apoptotic drug-induced iodide influx or taurine efflux, our data now strongly suggest that LRRC8 channels are involved in both RVD and AVD. Since disruption of the obligatory VRAC subunit LRRC8A also reduced the activation of caspase-3 by two pro-apoptotic stimuli, staurosporine and cisplatin, our results are compatible with the notion that apoptosis is facilitated by an LRRC8A-dependent volume decrease. The requirement for LRRC8D in cisplatin-induced, but not in staurosporine-induced caspase activation, can be explained by different mechanisms of cellular uptake. Staurosporine, a large hydrophobic compound that may cross membranes by passive diffusion, apparently does not enter cells through VRAC since it activated caspases regardless of whether it was applied in iso- or hypotonic medium. By contrast, cisplatin permeates through VRACs, in particular those containing LRRC8D subunits. This uptake mechanism imposes an additional LRRC8D dependence on caspase induction by cisplatin.

Cisplatin and carboplatin uptake through VRAC

Like $I_{Cl,vol}$ and taurine efflux (Voss *et al*, 2014), cellular cisplatin uptake was strongly stimulated by hypotonic swelling, as reported previously (Smith & Brock, 1989). This uptake component was abolished in *LRRC8A*$^{-/-}$ and *LRRC8(B,C,D,E)*$^{-/-}$ cells which do not express functional VRACs and was inhibited by the VRAC inhibitor carbenoxolone. Furthermore, caspase activation by cisplatin showed a similar dependence on LRRC8 isoforms and medium tonicity as cisplatin uptake as is expected for an intracellular effect of cisplatin. Our results, which were obtained with up to four different cell lines and several independent *LRRC8* knockout clones that excluded off-target effects, constitute overwhelming evidence that LRRC8 channels directly transport cisplatin and carboplatin.

About 50 to 70% of long-term isotonic cisplatin uptake was dependent on LRRC8D and LRRC8A, respectively. The uptake component remaining in *LRRC8A*$^{-/-}$ and *LRRC8(B,C,D,E)*$^{-/-}$ cells probably represents passive diffusion across the plasma membrane (Gately & Howell, 1993). The dependence on LRRC8D was surprising since this isoform is dispensable for $I_{Cl,vol}$ (Voss *et al*, 2014). Drug uptake through VRAC was also unexpected since this channel is thought to be closed under isotonic conditions (Nilius *et al*, 1997), which prevents a continuous loss of cellular constituents like amino acids. However, LRRC8-dependent isotonic uptake of cisplatin in HEK cells developed with a time course that was

Figure 6. LRRC8 subunit- and osmolarity-dependent carboplatin/cisplatin transport.

A Carboplatin uptake into control KBM7 cells and two LRRC8D-deficient clones (n = 6).

B Hypotonicity-stimulated cisplatin uptake in HEK WT cells was selectively blocked by 100 μM carbenoxolone (CBX), a non-specific blocker of VRAC (n = 3).

C, D Cisplatin uptake into HEK cells of indicated genotypes using 40 μM cisplatin under long-term isotonic (C) or 200 μM cisplatin in short-term hypo- and isotonic (D) conditions as function of time (n = 3). Similar results were obtained in HCT116 cells (Fig EV4).

E, F Cisplatin uptake (200 μM) into HEK cells of indicated genotypes. *LRRC8(B,C,E)*$^{-/-}$ and *LRRC8(B,D,E)*$^{-/-}$ cells express only LRRC8A and LRRC8D, and LRRC8A and LRRC8C, respectively (n = 3 for WT, 6 for *LRRC8D*$^{-/-}$, 9 for *LRRC8A*$^{-/-}$ in E; n = 3 in F).

G Mean current densities of maximally activated $I_{Cl,vol}$ at −80 mV. The number of cells is indicated for each column.

H Ratio of LRRC8-dependent swelling-activated cisplatin uptake (60 min) to mean $I_{Cl,vol}$ (as in G) as function of genotype.

Data information: Data are presented as mean ± SEM. *P < 0.05; **P < 0.01; and ***P < 0.001 (for (C, E) compared to *LRRC8A*$^{-/-}$ cells). Dotted lines in (D) and (F) highlight that there is no significant difference in isotonic 60-min uptake between the genotypes.

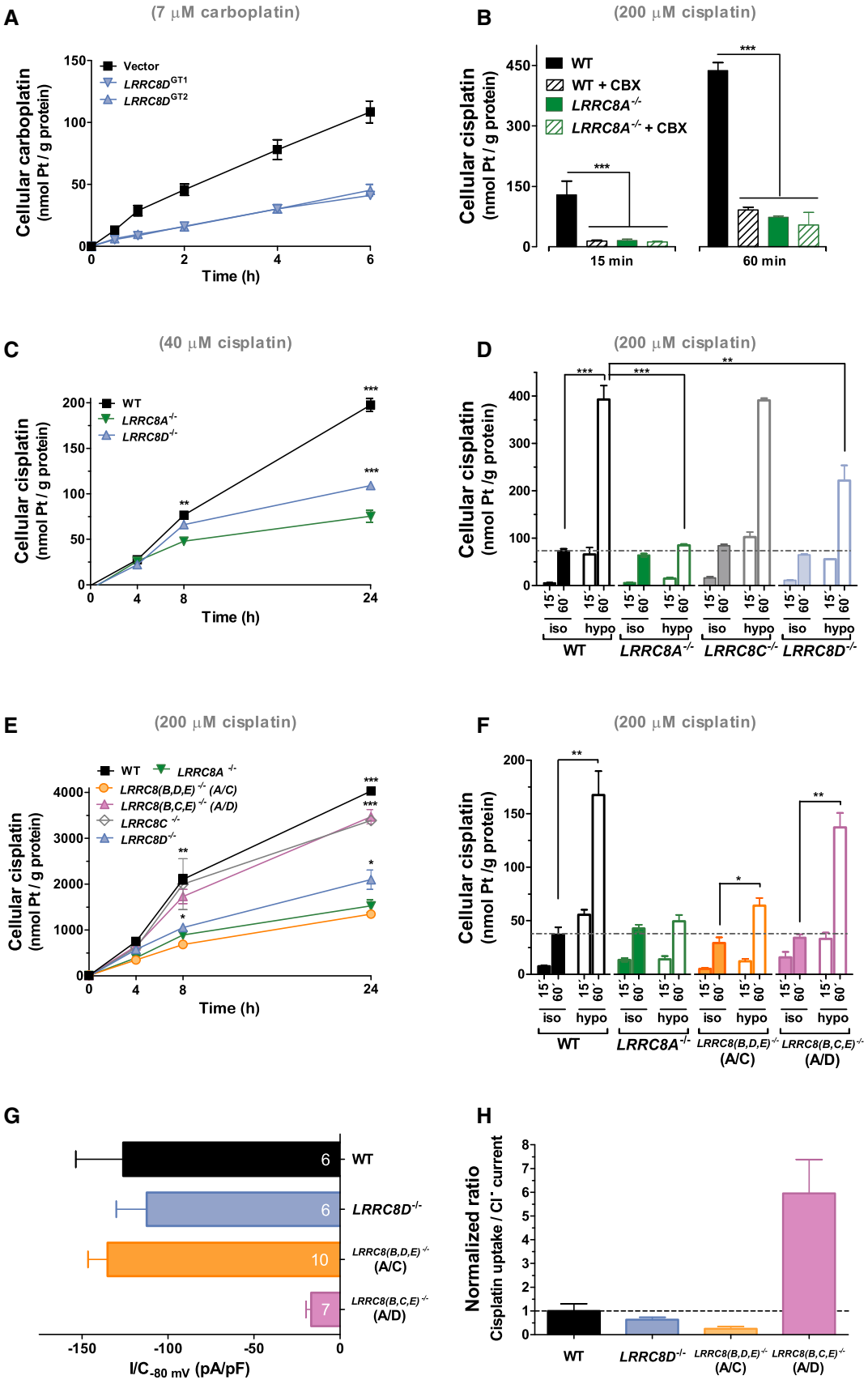
A
(7 μM carboplatin)
Cellular carboplatin (nmol Pt / g protein)
Vector
LRRC8D GT1
LRRC8D GT2
Time (h)
B
(200 μM cisplatin)
Cellular cisplatin (nmol Pt / g protein)
WT
WT + CBX
LRRC8A -/-
LRRC8A -/- + CBX
15 min
60 min
C
(40 μM cisplatin)
Cellular cisplatin (nmol Pt / g protein)
WT
LRRC8A -/-
LRRC8D -/-
Time (h)
D
(200 μM cisplatin)
Cellular cisplatin (nmol Pt /g protein)
iso
hypo
WT
LRRC8A -/-
LRRC8C -/-
LRRC8D -/-
E
(200 μM cisplatin)
Cellular cisplatin (nmol Pt / g protein)
WT
LRRC8A -/-
LRRC8(B,D,E) -/- (A/C)
LRRC8(B,C,E) -/- (A/D)
LRRC8C -/-
LRRC8D -/-
Time (h)
F
(200 μM cisplatin)
Cellular cisplatin (nmol Pt /g protein)
iso
hypo
WT
LRRC8A -/-
LRRC8(B,D,E) -/- (A/C)
LRRC8(B,C,E) -/- (A/D)
G
WT
LRRC8D -/-
LRRC8(B,D,E) -/- (A/C)
LRRC8(B,C,E) -/- (A/D)
I/C -80 mV (pA/pF)
H
Normalized ratio
Cisplatin uptake / Cl- current
WT
LRRC8D -/-
LRRC8(B,D,E) -/- (A/C)
LRRC8(B,C,E) -/- (A/D)

Figure 6.

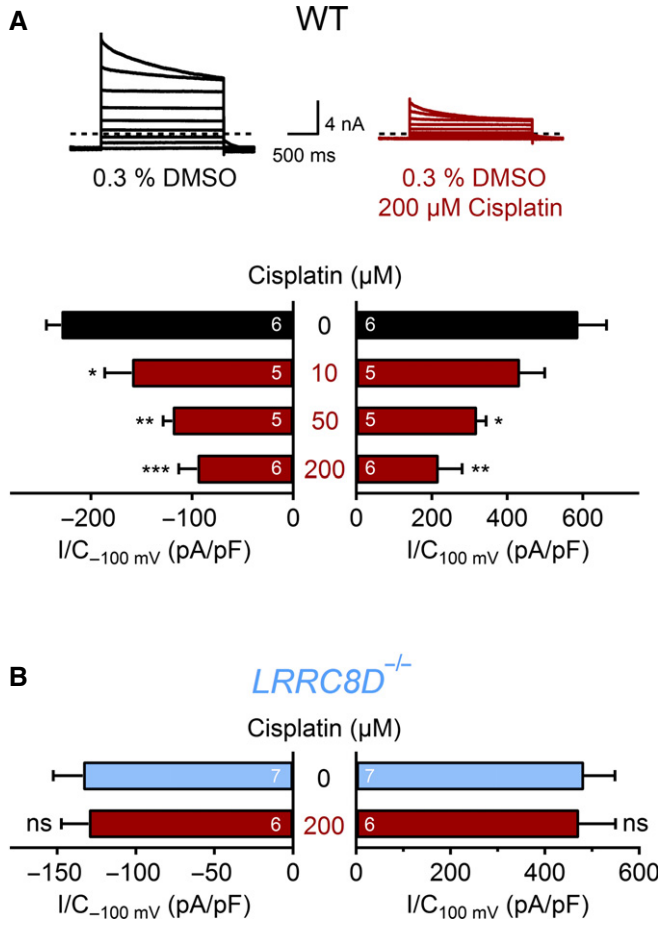

Figure 7. Cisplatin–DMSO inhibition of $I_{Cl,vol}$ depends on the LRRC8D subunit.

A Upper panel, example current traces (as in Fig 3A) of fully activated $I_{Cl,vol}$ in HEK cells exposed to hypotonic solution containing vehicle (0.3% DMSO) or 200 µM cisplatin in 0.3% DMSO. Dashed lines indicate zero current. Lower panel, $I_{Cl,vol}$ current densities (at −100 mV and 100 mV) of WT HEK cells treated with different cisplatin concentrations.

B No effect of 200 µM cisplatin/DMSO on $I_{Cl,vol}$ in *LRRC8D*$^{-/-}$ HEK cells.

Data information: Data are presented as mean ± SEM; the number of experiments is given for each bar; *P < 0.05; **P < 0.01.

consistent with a slow drug-induced activation of VRAC. Previously, the activation of *bona fide* VRAC channels or AVD by 5–15 µM cisplatin has been observed after time lags that ranged from ~20 min (Min *et al*, 2011; Cai *et al*, 2015) to ~4 h (Poulsen *et al*, 2010). The time course of drug-induced activation of LRRC8A-dependent iodide and taurine fluxes observed here is consistent with those previous findings. It appears that only a small fraction of VRAC is activated by pro-apoptotic stimuli because the observed iodide, taurine, and cisplatin transport rates were roughly an order of magnitude lower than those obtained with strong hypotonic stimuli. This fits the low VRAC current amplitudes observed by others (Shimizu *et al*, 2004) upon exposure of cells to pro-apoptotic drugs. Our data suggest that cisplatin, after having entered cells through passive diffusion across the plasma membrane, opens VRAC as an additional pathway for its uptake. This feedforward mechanism results in additional cisplatin-induced cisplatin uptake.

Dual role of LRRC8 in drug resistance: drug uptake and AVD-related apoptosis

Many biochemical alterations result in resistance to Pt-based anticancer drugs of cultured cells, but it has remained unclear which proteins are involved in medically relevant Pt drug transport (Borst *et al*, 2008; Hall *et al*, 2008; Burger *et al*, 2011; Ivy & Kaplan, 2013). We now identified VRAC as a major uptake mechanism for cis- and carboplatin. As VRACs mediated about half of isotonic cisplatin uptake, downregulation of LRRC8 subunits could have significant impact on tumor drug resistance. While requiring confirmation by prospective studies, this notion is supported by our analysis of two independent data sets from ovarian cancer patients: *LRRC8D* downregulation correlated with poor survival of Pt drug-treated patients. No correlation was seen with reduced *LRRC8A* expression, possibly because LRRC8A-dependent volume regulation is a viability factor for cells.

In addition to its role in cisplatin/carboplatin uptake, VRAC facilitated apoptosis through an independent, possibly AVD-related mechanism. An impairment of apoptosis may further contribute to drug resistance (Kelly & Strasser, 2011; Speirs *et al*, 2011), although tumor cells treated with therapeutic doses of Pt drugs probably die predominantly by other mechanisms (Borst *et al*, 2001; Brown & Wilson, 2003; Brown & Attardi, 2005). Acute induction of apoptosis in HCT116 cells, as analyzed in Fig 4, is thought to require cisplatin concentrations that are ~10-fold higher than therapeutic ones (Berndtsson *et al*, 2007). Such an induction is independent of nuclear DNA damage (Mandic *et al*, 2003) and depends on the production of reactive oxygen species (ROS) (Berndtsson *et al*, 2007) which can activate VRACs (Shimizu *et al*, 2004; Varela *et al*, 2004). Therefore, the relevance of VRAC-facilitated apoptosis at therapeutic doses remains to be determined in tumors of patients.

LRRC8D increases VRAC's permeability for cisplatin/carboplatin and taurine

Whereas the obligatory LRRC8A subunit is required for the surface expression of VRAC, no specific roles could be assigned so far to the other subunits, except for an influence on the kinetics of inactivation at non-physiological voltages (Voss *et al*, 2014). We have now discovered a role of LRRC8D in taurine and cisplatin/carboplatin transport that is biologically and medically important. Although *LRRC8D* disruption did not decrease swelling-activated Cl^- currents ($I_{Cl,vol}$) (Fig 3A and B; Voss *et al*, 2014), it reduced both isotonic and swelling-activated cisplatin uptake and blunted the ensuing activation of caspases. Comparison of swelling-induced cisplatin and Cl^- transport ($I_{Cl,vol}$) revealed that the incorporation of LRRC8D substantially increased VRAC's cisplatin/Cl^- transport ratio, as most strikingly demonstrated by the > 10-fold different transport ratio between LRRC8A/D and LRRC8A/C channels. The substantial swelling-activated cisplatin transport remaining in *LRRC8D*$^{-/-}$ cells (Figs 6D and EV4B) indicates that the cisplatin permeability of VRAC is not absolutely dependent on LRRC8D. LRRC8A/C and LRRC8A/E heteromers transported cisplatin very poorly under isotonic conditions (Figs 6E and EV5), but significant, albeit small, transport through A/C channels could be elicited by cell swelling (Fig 6F). Hence, even A/C channels may, in principle, transport

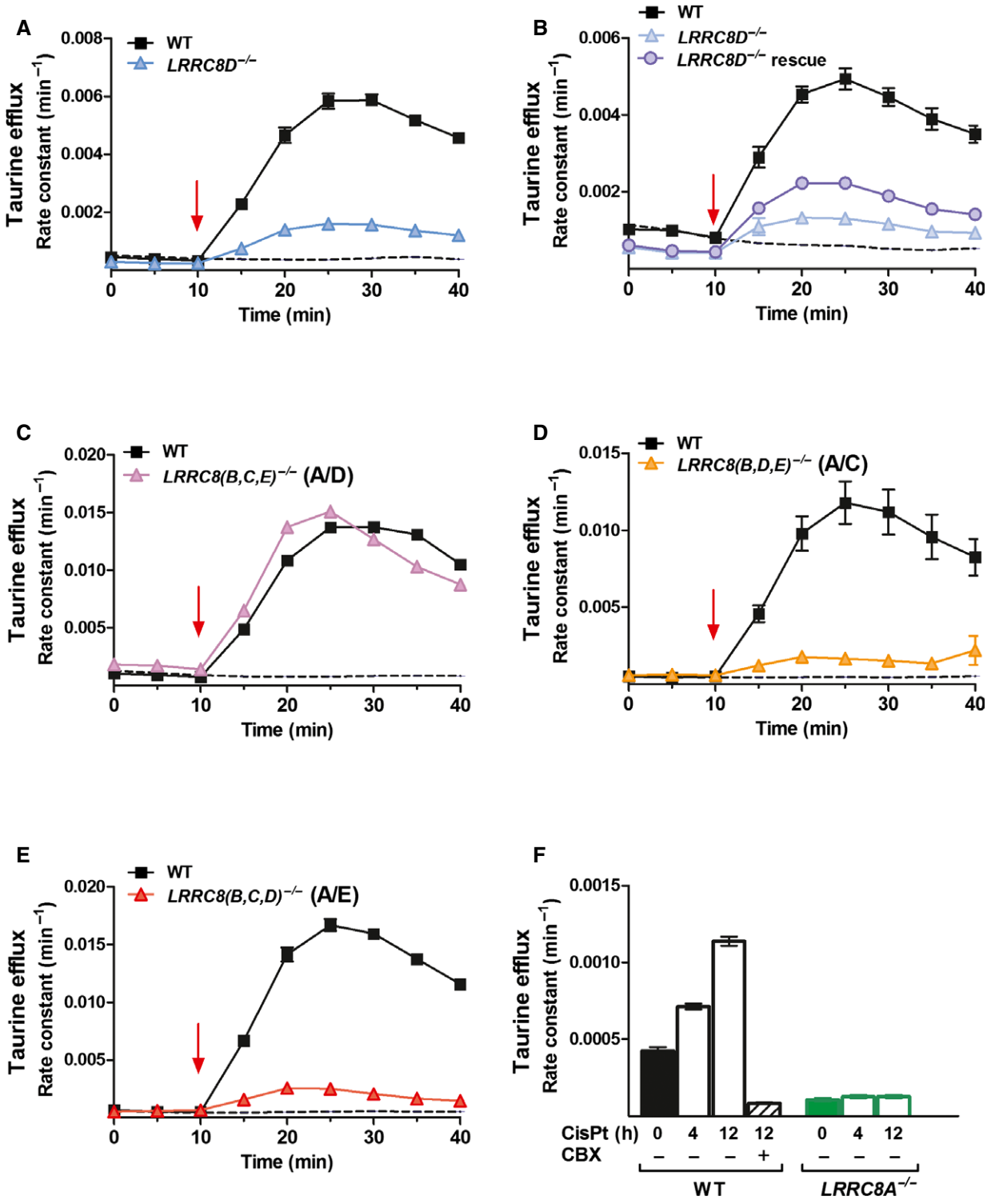

Figure 8. LRRC8A/LRRC8D-containing channels transport the cellular osmolyte taurine.

A, B Swelling-induced efflux of ^{3}[H]-taurine from WT and *LRRC8D*$^{-/-}$ HEK cells (A, B) and partial rescue by transient transfection of LRRC8D (B). Rescue is incomplete due to low transfection/expression efficiency of LRRC8D (Voss *et al*, 2014).

C–E Swelling-induced efflux of ^{3}[H]-taurine from *LRRC8(B,C,E)*$^{-/-}$ (C), *LRRC8(B,D,E)*$^{-/-}$ (D), or *LRRC8(B,C,D)*$^{-/-}$ (E) HEK cells compared to WT cells.

F Cisplatin-induced taurine efflux (over 30 min) from WT and *LRRC8A*$^{-/-}$ HEK cells after preincubation with 200 μM cisplatin for 4 or 12 h, or without cisplatin (0 h). Carbenoxolone (CBX; 100 μM) blocks taurine efflux from WT cells treated for 12 h with cisplatin, excluding taurine flux through unspecific leaks.

Data information: Data are presented as mean ± SEM. Dashed lines in (A–E) represent isotonic efflux from the same individual experiments. Red arrows, change to hypotonic solution. Each panel shows the average of two independent experiments (n = 4 for each experiments, i.e., n = 8 in total).

cisplatin. Possible roles of other subunits and subunit combinations remain to be explored.

A mere loss of LRRC8D-containing, cisplatin-preferring channels should have quantitatively similar effects on isotonic and hypotonic uptake. However, whereas under long-term isotonic conditions, *LRRC8D* disruption reduced the LRRC8-dependent component (as defined by the difference between WT and *LRRC8A*$^{-/-}$ cells) by ~70%, the hypotonicity-stimulated cisplatin uptake component was diminished by only ~50% or less in *LRRC8D*$^{-/-}$ cells. This disparity suggests a differential activation of LRRC8D-containing heteromers by pro-apoptotic drugs or cell swelling.

LRRC8D also plays a prominent physiological role. It crucially determines VRAC's taurine permeability, but mirroring its role in cisplatin transport, it is not absolutely required for taurine transport. Taurine, the cellular concentrations of which range from 5 to 50 mM, is an important cellular osmolyte and has several additional biological roles (Lambert *et al*, 2015). *LRRC8D*$^{-/-}$ cells can now be used to estimate the contribution of organic osmolytes to cell volume regulation. Our RVD experiments suggest that this contribution is substantial. The simultaneous presence in the plasma membrane of VRACs incorporating or lacking LRRC8D subunits probably explains previous observations which suggested that the volume-regulated anion channel VRAC is molecularly distinct from a volume-sensitive organic osmolyte and anion channel VSOAC (Lambert & Hoffmann, 1994; Stutzin *et al*, 1999; Shennan, 2008).

Implications for the pore of VRACs

The dependence of the substrate selectivity on subunit composition is compelling evidence that LRRC8 heteromers form the VRAC pore. The structural basis of VRAC selectivity is currently unknown. Remarkably, VRACs are thought to display a substantial anion > cation selectivity for inorganic ions (Nilius *et al*, 1997), while also transporting rather large organic substrates. The radius of the VRAC pore has been estimated to be 0.6–0.7 nm (Droogmans *et al*, 1999; Ternovsky *et al*, 2004). This value is compatible with the release of organic osmolytes like taurine and amino acids and also with the uptake of cisplatin and carboplatin (maximal radius of ~0.15 and ~0.28 nm, respectively). On the other hand, this simple consideration does not explain the observation that oxaliplatin ($r \sim 0.45$ nm) did not permeate, whereas blasticidin S ($r \sim 0.7$ nm) apparently does (Lee *et al*, 2014).

The conundrum of a highly halide-selective pore that also conducts much larger and differently charged organic substrates rests on the assumption that there is just one VRAC, and not a whole spectrum of differently composed LRRC8 heteromers, that is, different VRACs. Given the wide tissue distribution of most LRRC8 isoforms, it is likely that various VRACs with diverse properties are co-expressed in the same cell. Our work is compatible with the possibility that some subunit combinations form channels that only conduct organic substrates, whereas others only conduct small anions. However, since, for example, *LRRC8(B,C,E)*$^{-/-}$ cells transport both organic molecules and Cl^-, this hypothesis demands that LRRC8A and LRRC8D can assemble with different stoichiometries and thereby yield channels with different substrate selectivities. This proposition, which could apply for other subunit combinations as well, is difficult to test.

Our work revealed that the specific subunit composition of VRACs determines their substrate specificity, regulation, and pharmacology. LRRC8A/LRRC8D-containing VRACs, which are amenable to specific pharmacological modulation, are important for cell volume regulation by organic osmolytes. They may also play an important dual role in tumor drug sensitivity by mediating cisplatin/carboplatin uptake and possibly by modulating the progression of apoptosis.

Materials and Methods

Loss-of-function screens

A haploid-genetic screen for carboplatin resistance was performed as described (Carette *et al*, 2011). 10^8 KBM7 cells were transduced with a gene-trap retrovirus using spin infection. 10^8 mutagenized cells were then exposed to 7 μM carboplatin and distributed over 96-well plates (10^5 cells/well). Surviving clones were pooled after 21 days and subjected to density centrifugation using lymphocyte separation medium (Lonza, 30 min at 400 *g*) to remove cell debris. Next, 3×10^7 cells were pelleted for genomic DNA isolation (QiaAmp DNA mini kit, Qiagen). Gene-trap insertion sites were amplified by inverse PCR. First, genomic DNA was digested using the restriction enzymes NlaIII and MseI (New England Biolabs) overnight at 37°C. Fragments were then circularized using T4 DNA ligase (New England Biolabs) (o/n at RT). Fragments containing the gene-trap sequence and flanking genomic DNA were amplified by PCR using primers containing the Illumina adapters P5 and P7 (for NlaIII-digested DNA: 5′-AATGATACGGCGACCACCGAGATCTGATGGTTCTCTAGCTTGCC-3′ and 5′-CAAGCAGAAGACGGCATACGACCCAGGTTAAGATCAAGGTC-3′; for MseI-digested DNA: 5′-AATGATACGGCGACCACCGAGATCTGATGGTTCTCTAGCTTGCC-3′ and 5′-CAAGCAGAAGACGGCATACGACGTTCTGTGTTGTCTCTGTCTG-3′).

Products were purified (PCR purification kit, Qiagen) and sequenced on a HiSeq 2000 (Illumina) using a custom sequencing primer 5′-CTAGCTTGCCAAACCTACAGGTGGGGTCTTTCA-3′.

Sequence reads were cropped to 36 bp for comparability with previously performed screens and aligned to the human genome (hg18) using bowtie (Langmead *et al*, 2009). Only reads that align uniquely without mismatches were considered. Additionally, reads aligning non-uniquely when 1 to 3 mismatches were allowed were removed, as well as reads falling within 2-bp distance of each other. As the gene-trap construct is unidirectional, only insertion sites in the sense orientation of intronic regions, and integrations in sense or antisense of exonic sequences were considered. To identify genes enriched in mutations following carboplatin treatment, the number of insertion sites per gene was compared to an unselected mutagenized population (Carette *et al*, 2011) using a one-sided Fisher exact test. Correction for multiple testing for *P*-values was carried out using Benjamini and Hochberg FDR correction in R.

Cytotoxicity and colony formation assays

LRRC8D-expressing and LRRC8D-deficient KBM7 cells were seeded in 96-well plates in triplicates (3×10^5 cells per well) and treated with various concentrations of carboplatin, cisplatin, and oxaliplatin for 96 h. Relative numbers of viable cells were measured in

comparison with the untreated control and the solvent control using the fluorimetrical, resazurin-based Cell Titer Blue® assay (Promega). Measurements were performed according to the manufacturer's instructions at 560Ex/590Em nm in a Tecan counter (Infinite M200). Cell growth was expressed as percentage of the untreated control.

Regarding HAP1 cells, 10,000 *LRRC8A*$^{-/-}$ HAP1 and 8,000 HAP1 vector control cells were seeded per well into 6-well plates to account for differences in growth rate. Cells were assayed for colony formation in the presence of five different concentrations of carboplatin, cisplatin, or oxaliplatin. After 7 days, surviving colonies were formalin-fixed and stained with crystal violet. The optical absorption was determined at 590 nm after extracting the dye with 10% acetic acid.

LRRC8 knockout cell lines

The generation of stably diploid HCT116 cells and polyploid HEK293 cells with disruptions in one or several *LRRC8* genes using the CRISPR-Cas9 method has been described previously (Voss *et al*, 2014). HEK cells lacking LRRC8A-E singly or in various combinations, and HAP1 cells lacking LRRC8A or LRRC8D, were newly generated using the same procedure. KBM7 clones lacking LRRC8D were obtained from Hidde Ploegh (Lee *et al*, 2014). Disruption of *LRRC8* genes was confirmed by genomic sequencing and Western blotting (Fig EV1).

Antibodies and Western blots

Polyclonal rabbit antibodies against LRRC8A and LRRC8E have been described previously (Voss *et al*, 2014). New antibodies were raised against LRRC8B, LRRC8C and LRRC8D in rabbits using the following peptides that were coupled through N-terminally added cysteines to keyhole limpet hemocyanin: QSLPYPQPGLESPGIESPT, LRRC8B; EDALFETLPSDVREQMKAD, LRRC8C; LEVKEALNQDVN VPFANGI, LRRC8D. Sera were purified by affinity to the respective peptides. Western blots of native HCT116 and HEK cells, together with cells lacking the respective LRRC8 isoforms, confirmed the specificity of the antisera, even though some sera (α-LRRC8C, α-LRRC8D) were made against mouse peptide sequences that differed by a few amino acids from the human counterparts. Western blots were done following standard procedures using antibodies against tubulin or actin as loading controls.

Electrophysiology

VRAC-mediated swelling-activated anion currents $I_{Cl,vol}$ were measured in the whole-cell patch-clamp configuration as described (Voss *et al*, 2014). Cells were swollen by exposure to hypotonic solution (240 mOsm) that differed from the isotonic solution (320 mOsm: 150 NaCl, 6 KCl, 1 $MgCl_2$, 1.5 $CaCl_2$, 10 glucose, and 10 HEPES, pH 7.4) by containing 105 instead of 150 mM NaCl. In order to isolate Cl^- currents, the pipette solution contained (in mM) the following: 40 CsCl, 100 Cs-methanesulfonate, 1 $MgCl_2$, 1.9 $CaCl_2$, 5 EGTA, 4 Na_2ATP, and 10 HEPES, pH 7.2 (290 mOsm). Whole-cell currents were monitored by voltage ramps from −100 to +100 mV and voltage-clamp traces recorded using the protocol shown in Fig 3A.

Measurement of regulatory volume decrease (RVD)

Cell volume regulation was measured semiquantitatively using the calcein method (Capó-Aponte *et al*, 2005) in a fluorometric imaging plate reader (FLIPR^{TM}; Molecular Devices) in a 384-well format as described (Voss *et al*, 2014). Cell swelling was initiated by decreasing extracellular osmolarity to 94 mOsm, and calcein fluorescence was followed at λ = 515–575 nm for ~65 min.

Drug-induced iodide influx

Iodide influx into HEK cells expressing an iodide-sensitive YFP variant (Galietta *et al*, 2001) was carried out using the FLIPR^{TM} as described (Voss *et al*, 2014), but using both *LRRC8A*$^{+/+}$ and *LRRC8A*$^{-/-}$ cells. Cells in half of the wells of 384-well plates were preincubated with 4 μM staurosporine (in 0.4% DMSO; also added to control wells) or 200 μM cisplatin (without DMSO) for the times indicated in Fig 7. Iodide uptake (always under isotonic conditions) was initiated by pipetting 25 μl of a solution containing 70 mM iodide to the well, resulting in a final iodide concentration of 50 mM. YFP quenching was followed over time using illumination at λ = 495–505 nm and fluorescence measurement at λ = 526–585 nm using the Fluo3 LED/filter set. Maximal fluorescence quenching rates were determined as semiquantitative measure of iodide uptake. Values were averaged from 16 wells for each condition.

Caspase-3 activity determination

Cells covering (~90% confluency) the bottom of 6-cm plates were incubated at 37°C/5% CO_2 in DMEM/FCS containing 4 μM staurosporine, or 0.4% DMSO as vehicle control, or 200 μM cisplatin (without DMSO). Cells were collected at different times of drug exposure. To explore the dependence on osmolarity, cells were incubated with 4 μM staurosporine or 200 μM cisplatin in isotonic (320 mOsm) or hypotonic (240 mOsm) solution (as described for electrophysiology) for 1 h at 37°C. The drug-containing solutions were then replaced by normal medium and cells incubated for different times. Caspase activity from cytosolic extracts was monitored fluorometrically in a Safire2 plate reader (Tecan AG, CH) set at 37°C using as substrate 30 μM Ac-DEVD-AMC (Enzo). Specific enzymatic activity was calculated from the slopes of the best fit curves and normalized to total protein. For long-term isotonic protocols, the activity was further normalized to "time zero" samples.

Measurement of taurine efflux

HEK293 cells were grown to ~80% confluency (48–72 h after plating) in 35-mm diameter plates coated with poly-L-lysine. For rescue experiments, cells were transfected one day before flux measurements with an LRRC8D expression plasmid using Fugene HD. WT and *LRRC8D*$^{-/-}$ control cells were mock transfected with a GFP expression vector. Cells were loaded with ^{3}[H]-taurine (2 μCi/ml; Hartmann Analytics) for 2 to 2.5 h in culture medium (without FCS) at 37°C. They were then washed five times at room temperature with isotonic solution (same as used in electrophysiology). After washing, external media were removed in 5-min intervals and replaced with fresh isotonic or hypotonic solution (same as in electrophysiology) and saved for counting. To measure cisplatin-induced

taurine efflux, cells were preincubated with cisplatin (200 μM) in cell culture medium for 2 or 10 h. Cells were then loaded with ^{3}[H]-taurine for 2 h in cell culture medium (±200 μM cisplatin, w/o FCS and w/o DMSO) at 37°C. Cells were washed 5 times and incubated for 30 min at 37°C with fresh isotonic solution. As a control for LRRC8 contribution to cisplatin-induced taurine efflux, isotonic solution containing 100 μM carbenoxolone was used throughout the washes. At the end of the experiments, cells were lysed with 0.75 ml of 0.1 M NaOH. The radioactivity of cell supernatants and of the final cell lysate was determined in a liquid scintillation counter. Rate constants were calculated as previously described (Holm *et al*, 2013).

Uptake of cisplatin into cells

Intracellular platinum drug concentrations were measured as described (Brouwers *et al*, 2005) or by ICP-MS (Brouwers *et al*, 2006) (NKI and Institut für Medizinische Diagnostik (IMD), Berlin). Cells in 6-cm plates (~90% confluency) were incubated at 37°C/5% CO_2 in DMEM/FCS containing cisplatin (without DMSO) for different times as indicated. For determining the dependence of uptake on osmolarity, cells were incubated with 200 μM cisplatin in isotonic or hypotonic solution (same as used in electrophysiology) for the indicated time periods at 37°C. At the end of the uptake period, cells were quickly washed 5 times with 3 ml ice-cold PBS, collected, gently spun down (1,000 *g*, 5 min, 4°C), and the pellet was resuspended in 0.1 M HCl. For carboplatin uptake in KBM7 cells grown in suspension, 2×10^7 cells per group (in T25 flasks) were incubated at 37°C/5% CO_2 in IMDM Glutamax (10% FBS) containing 7 μM carboplatin (without DMSO) and samples were collected at the indicated time points after drug treatment. Cells were quickly washed twice with 10 ml cold PBS (400 *g*, 5 min), and the pellet was resuspended in 1 ml cold PBS. Of this suspension, 100 μl was taken for protein concentration determination using the BCA assay. The rest (900 μl) was spun down (400 *g*, 5 min) and resuspended in 200 μl 0.1 M HCL for ICP-MS.

Statistics

Data are presented as mean ± SEM, with *n* denoting the number of observations (samples). For RVD measurements (Fig 3C), cisplatin uptake in Figs 6C–F and EV4, caspase induction (Fig 4A), activation of VRAC iodide flux (Fig 5), and Western blots (Fig EV1), a minimum of two independent experiments were performed with similar results. Student's *t*-tests for paired or unpaired data were employed as appropriate and considered as significant as follows: $^{*}P < 0.05$; $^{**}P < 0.01$; and $^{***}P < 0.001$.

Gene expression and survival analysis based on published data concerning ovarian cancer patients

Gene expression data were downloaded from the TCGA (http://cancergenome.nih.gov/). The expression data are derived from RNAseq with expression quantification using RSEM. The density plot shows the log of the gene expression of the individual LRRC8 family members. The survival analysis uses the clinical data provided by the TCGA. The number of days to death is scored as an event. As time interval definition, we used "days_to_last_follow-up." This is the time interval from the date of last follow-up to the date of initial pathologic diagnosis, represented as a calculated number of days (https://tcga-data.nci.nih.gov/docs/dictionary/). The patients were stratified on the expression levels of *LRRC8A* or *LRRC8D*. Those that were in the lowest tertile (< 33%) of the levels were classed as having low expression. The analysis is performed with the package "survival" from the R-project.

The Australian ovarian cancer (OV AU) expression data of the study performed by Patch *et al* (2015) were gene-wise matched to the TCGA panel after which the selected RSEM was normalized. A survival analysis was performed contrasting the low (< 33%) expression of *LRRC8A* or *LRRC8D* against the rest.

Expanded View for this article is available online.

Acknowledgements
We thank Carolin Backhaus, Andrea Weidlich, and Janet Liebold for technical assistance, and Martin Neuenschwander, Silke Radetzki, and Jens von Kries of the FMP Screening Unit for collaboration in the VRAC compound screen that identified cisplatin–DMSO adducts as VRAC inhibitors. We are grateful to Hidde Ploegh (Whitehead Institute for Biomedical Research, Cambridge, USA) for providing the LRRC8D^{GT1} and LRRC8D^{GT2} cells. Olaf van Tellingen (NKI), Jos Beijnen, Hilde Rosing, Niels de Vries, and Matthijs Tibben (NKI/Slotervaart hospital) were very helpful with platinum measurements. This work was supported by the European Research Council Advanced Grant (FP/2007-2013) 294435 "Cytovolion" and the Deutsche Forschungsgemeinschaft (Exc 257 "NeuroCure") to T.J.J., the Netherlands Organization for Scientific Research (NWO-VIDI 016.116.302) to S.R, and the Swiss National Science Foundation (P1BEP3_155461) to N.M.G.

Author contributions
RPC planned, performed, and analyzed experiments (cisplatin uptake (HEK and HCT116 cells), caspase induction, Western blots, iodide influx, cell volume regulation) and wrote the paper; DL generated HEK LRRC8 KO cell lines and performed and analyzed taurine flux experiments; CG performed and analyzed haploid cell resistance screens and KBM7 cytotoxicity assays; NMG and AK performed and analyzed KBM7 cytotoxicity assays, HAP1 clonogenic assays, and Pt uptake into haploid cells; AK measured cellular Pt concentrations; FU and SMR performed and analyzed electrophysiological experiments; DAE performed cisplatin uptake (HEK and HCT116); GX performed and analyzed KBM7 Pt uptake experiments; FKV performed and analyzed cell volume regulation and iodide influx experiments; TS analyzed LRRC8 antibodies; VAB analyzed haploid screens; DJV and LFW performed cancer database analysis; TRB planned and advised on haploid screens; PB advised, analyzed experiments, and wrote the paper; SR planned and analyzed experiments and wrote the paper; TJJ planned and analyzed experiments and wrote the paper. All authors read and commented on the paper.

Conflict of interest
The authors declare that they have no conflict of interest.

References

Abascal F, Zardoya R (2012) LRRC8 proteins share a common ancestor with pannexins, and may form hexameric channels involved in cell-cell communication. *BioEssays* 34: 551 – 560

d'Anglemont de Tassigny A, Berdeaux A, Souktani R, Henry P, Ghaleb B (2008) The volume-sensitive chloride channel inhibitors prevent both contractile dysfunction and apoptosis induced by doxorubicin through PI3kinase, Akt and Erk 1/2. *Eur J Heart Fail* 10: 39 – 46

Berndtsson M, Hagg M, Panaretakis T, Havelka AM, Shoshan MC, Linder S (2007) Acute apoptosis by cisplatin requires induction of reactive oxygen species but is not associated with damage to nuclear DNA. *Int J Cancer* 120: 175 – 180

Borst P, Borst J, Smets LA (2001) Does resistance to apoptosis affect clinical response to antitumor drugs? *Drug Resist Updat* 4: 129 – 131

Borst P, Rottenberg S, Jonkers J (2008) How do real tumors become resistant to cisplatin? *Cell Cycle* 7: 1353 – 1359

Brouwers EE, Tibben MM, Joerger M, van Tellingen O, Rosing H, Schellens JH, Beijnen JH (2005) Determination of oxaliplatin in human plasma and plasma ultrafiltrate by graphite-furnace atomic-absorption spectrometry. *Anal Bioanal Chem* 382: 1484 – 1490

Brouwers EE, Tibben MM, Rosing H, Hillebrand MJ, Joerger M, Schellens JH, Beijnen JH (2006) Sensitive inductively coupled plasma mass spectrometry assay for the determination of platinum originating from cisplatin, carboplatin, and oxaliplatin in human plasma ultrafiltrate. *J Mass Spectrom* 41: 1186 – 1194

Brown JM, Wilson G (2003) Apoptosis genes and resistance to cancer therapy: what does the experimental and clinical data tell us? *Cancer Biol Ther* 2: 477 – 490

Brown JM, Attardi LD (2005) The role of apoptosis in cancer development and treatment response. *Nat Rev Cancer* 5: 231 – 237

Burger H, Loos WJ, Eechoute K, Verweij J, Mathijssen RH, Wiemer EA (2011) Drug transporters of platinum-based anticancer agents and their clinical significance. *Drug Resist Updat* 14: 22 – 34

Cai S, Zhang T, Zhang D, Qiu G, Liu Y (2015) Volume-sensitive chloride channels are involved in cisplatin treatment of osteosarcoma. *Mol Med Rep* 11: 2465 – 2470

Capó-Aponte JE, Iserovich P, Reinach PS (2005) Characterization of regulatory volume behavior by fluorescence quenching in human corneal epithelial cells. *J Membr Biol* 207: 11 – 22

Carette JE, Guimarães CP, Varadarajan M, Park AS, Wuethrich I, Godarova A, Kotecki M, Cochran BH, Spooner E, Ploegh HL, Brummelkamp TR (2009) Haploid genetic screens in human cells identify host factors used by pathogens. *Science* 326: 1231 – 1235

Carette JE, Guimarães CP, Wuethrich I, Blomen VA, Varadarajan M, Sun C, Bell G, Yuan B, Muellner MK, Nijman SM, Ploegh HL, Brummelkamp TR (2011) Global gene disruption in human cells to assign genes to phenotypes by deep sequencing. *Nat Biotechnol* 29: 542 – 546

Droogmans G, Maertens C, Prenen J, Nilius B (1999) Sulphonic acid derivatives as probes of pore properties of volume-regulated anion channels in endothelial cells. *Br J Pharmacol* 128: 35 – 40

Fayad W, Brnjic S, Berglind D, Blixt S, Shoshan MC, Berndtsson M, Olofsson MH, Linder S (2009) Restriction of cisplatin induction of acute apoptosis to a subpopulation of cells in a three-dimensional carcinoma culture model. *Int J Cancer* 125: 2450 – 2455

Fischer SJ, Benson LM, Fauq A, Naylor S, Windebank AJ (2008) Cisplatin and dimethyl sulfoxide react to form an adducted compound with reduced cytotoxicity and neurotoxicity. *Neurotoxicology* 29: 444 – 452

Galietta LJ, Haggie PM, Verkman AS (2001) Green fluorescent protein-based halide indicators with improved chloride and iodide affinities. *FEBS Lett* 499: 220 – 224

Gately DP, Howell SB (1993) Cellular accumulation of the anticancer agent cisplatin: a review. *Br J Cancer* 67: 1171 – 1176

Hall MD, Okabe M, Shen DW, Liang XJ, Gottesman MM (2008) The role of cellular accumulation in determining sensitivity to platinum-based chemotherapy. *Annu Rev Pharmacol Toxicol* 48: 495 – 535

Hoffmann EK, Lambert IH (2014) Ion channels and transporters in the development of drug resistance in cancer cells. *Philos Trans R Soc Lond* 369: 20130109

Holm JB, Grygorczyk R, Lambert IH (2013) Volume-sensitive release of organic osmolytes in the human lung epithelial cell line A549: role of the 5-lipoxygenase. *Am J Physiol Cell Physiol* 305: C48 – C60

Hyzinski-García MC, Rudkouskaya A, Mongin AA (2014) LRRC8A protein is indispensable for swelling-activated and ATP-induced release of excitatory amino acids in rat astrocytes. *J Physiol* 592: 4855 – 4862

Ise T, Shimizu T, Lee EL, Inoue H, Kohno K, Okada Y (2005) Roles of volume-sensitive Cl^- channel in cisplatin-induced apoptosis in human epidermoid cancer cells. *J Membr Biol* 205: 139 – 145

Ivy KD, Kaplan JH (2013) A re-evaluation of the role of hCTR1, the human high-affinity copper transporter, in platinum-drug entry into human cells. *Mol Pharmacol* 83: 1237 – 1246

Jackson PS, Strange K (1993) Volume-sensitive anion channels mediate swelling-activated inositol and taurine efflux. *Am J Physiol* 265: C1489 – C1500

Kelland L (2007) The resurgence of platinum-based cancer chemotherapy. *Nat Rev Cancer* 7: 573 – 584

Kelly GL, Strasser A (2011) The essential role of evasion from cell death in cancer. *Adv Cancer Res* 111: 39 – 96

Lambert IH, Hoffmann EK (1994) Cell swelling activates separate taurine and chloride channels in Ehrlich mouse ascites tumor cells. *J Membr Biol* 142: 289 – 298

Lambert IH, Kristensen DM, Holm JB, Mortensen OH (2015) Physiological role of taurine - from organism to organelle. *Acta Physiol (Oxf)* 213: 191 – 212

Lang F, Hoffmann EK (2012) Role of ion transport in control of apoptotic cell death. *Compr Physiol* 2: 2037 – 2061

Langmead B, Schatz MC, Lin J, Pop M, Salzberg SL (2009) Searching for SNPs with cloud computing. *Genome Biol* 10: R134

Lee EL, Shimizu T, Ise T, Numata T, Kohno K, Okada Y (2007) Impaired activity of volume-sensitive Cl^- channel is involved in cisplatin resistance of cancer cells. *J Cell Physiol* 211: 513 – 521

Lee CC, Freinkman E, Sabatini DM, Ploegh HL (2014) The protein synthesis inhibitor blasticidin S enters mammalian cells via leucine-rich repeat-containing protein 8D. *J Biol Chem* 289: 17124 – 17131

Maeno E, Ishizaki Y, Kanaseki T, Hazama A, Okada Y (2000) Normotonic cell shrinkage because of disordered volume regulation is an early prerequisite to apoptosis. *Proc Natl Acad Sci USA* 97: 9487 – 9492

Mandic A, Hansson J, Linder S, Shoshan MC (2003) Cisplatin induces endoplasmic reticulum stress and nucleus-independent apoptotic signaling. *J Biol Chem* 278: 9100 – 9106

Min XJ, Li H, Hou SC, He W, Liu J, Hu B, Wang J (2011) Dysfunction of volume-sensitive chloride channels contributes to cisplatin resistance in human lung adenocarcinoma cells. *Exp Biol Med* 236: 483 – 491

Nilius B, Eggermont J, Voets T, Buyse G, Manolopoulos V, Droogmans G (1997) Properties of volume-regulated anion channels in mammalian cells. *Prog Biophys Mol Biol* 68: 69 – 119

Okada Y (1997) Volume expansion-sensing outward-rectifier Cl^- channel: fresh start to the molecular identity and volume sensor. *Am J Physiol* 273: C755 – C789

Okada Y, Shimizu T, Maeno E, Tanabe S, Wang X, Takahashi N (2006) Volume-sensitive chloride channels involved in apoptotic volume decrease and cell death. *J Membr Biol* 209: 21 – 29

Orlov SN, Platonova AA, Hamet P, Grygorczyk R (2013) Cell volume and monovalent ion transporters: their role in cell death machinery triggering and progression. *Am J Physiol Cell Physiol* 305: C361 – C372

Patch AM, Christie EL, Etemadmoghadam D, Garsed DW, George J, Fereday S, Nones K, Cowin P, Alsop K, Bailey PJ, Kassahn KS, Newell F, Quinn MC, Kazakoff S, Quek K, Wilhelm-Benartzi C, Curry E, Leong HS, Hamilton A, Mileshkin L *et al* (2015) Whole-genome characterization of chemoresistant ovarian cancer. *Nature* 521: 489 – 494

Pedersen SF, Klausen TK, Nilius B (2015) The identification of VRAC (Volume Regulated Anion Channel): an amazing Odyssey. *Acta Physiol (Oxf)* 213: 868 – 881

Poulsen KA, Andersen EC, Hansen CF, Klausen TK, Hougaard C, Lambert IH, Hoffmann EK (2010) Deregulation of apoptotic volume decrease and ionic movements in multidrug-resistant tumor cells: role of chloride channels. *Am J Physiol Cell Physiol* 298: C14 – C25

Qiu Z, Dubin AE, Mathur J, Tu B, Reddy K, Miraglia LJ, Reinhardt J, Orth AP, Patapoutian A (2014) SWELL1, a plasma membrane protein, is an essential component of volume-regulated anion channel. *Cell* 157: 447 – 458

Shennan DB (2008) Swelling-induced taurine transport: relationship with chloride channels, anion-exchangers and other swelling-activated transport pathways. *Cell Physiol Biochem* 21: 15 – 28

Shimizu T, Numata T, Okada Y (2004) A role of reactive oxygen species in apoptotic activation of volume-sensitive Cl^- channel. *Proc Natl Acad Sci USA* 101: 6770 – 6773

Smith E, Brock AP (1989) The effect of reduced osmolarity on platinum drug toxicity. *Br J Cancer* 59: 873 – 875

Sørensen BH, Thorsteinsdottir UA, Lambert IH (2014) Acquired cisplatin resistance in human ovarian A2780 cancer cells correlates with shift in taurine homeostasis and ability to volume regulate. *Am J Physiol Cell Physiol* 307: C1071 – C1080

Speirs CK, Hwang M, Kim S, Li W, Chang S, Varki V, Mitchell L, Schleicher S, Lu B (2011) Harnessing the cell death pathway for targeted cancer treatment. *Am J Cancer Res* 1: 43 – 61

Stutzin A, Torres R, Oporto M, Pacheco P, Eguiguren AL, Cid LP, Sepúlveda FV (1999) Separate taurine and chloride efflux pathways activated during regulatory volume decrease. *Am J Physiol* 277: C392 – C402

Ternovsky VI, Okada Y, Sabirov RZ (2004) Sizing the pore of the volume-sensitive anion channel by differential polymer partitioning. *FEBS Lett* 576: 433 – 436

Varela D, Simon F, Riveros A, Jørgensen F, Stutzin A (2004) NAD(P)H oxidase-derived H_2O_2 signals chloride channel activation in cell volume regulation and cell proliferation. *J Biol Chem* 279: 13301 – 13304

Voss FK, Ullrich F, Münch J, Lazarow K, Lutter D, Mah N, Andrade-Navarro MA, von Kries JP, Stauber T, Jentsch TJ (2014) Identification of LRRC8 heteromers as an essential component of the volume-regulated anion channel VRAC. *Science* 344: 634 – 638

Ye ZC, Oberheim N, Kettenmann H, Ransom BR (2009) Pharmacological "cross-inhibition" of connexin hemichannels and swelling activated anion channels. *Glia* 57: 258 – 269

Expanded View Figures

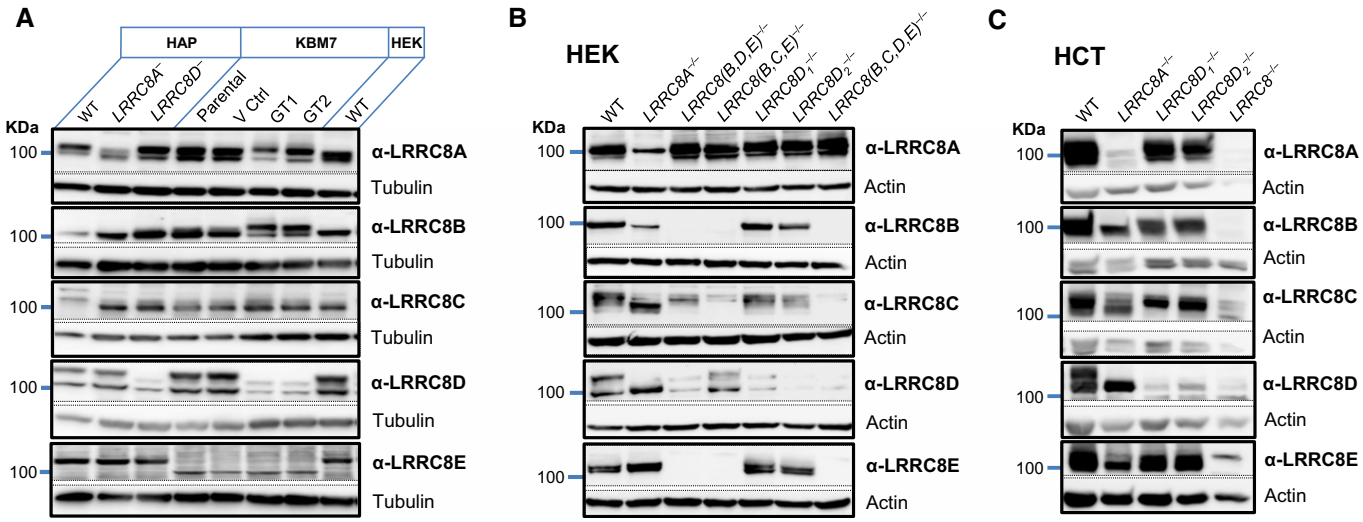

Figure EV1. LRRC8 subunit expression in different cell lines.

A–C Western blot showing the expression of all LRRC8 subunits in HAP1 and KBM7 (A), HEK (B), and HCT116 (C) cell lines, including knockout cell lines. Tubulin or actin was used as loading control. Note that KBM7 cells virtually lack LRRC8E, explaining the lack of inactivation of their $I_{Cl,vol}$ at clamped voltages (Fig 3B). Notice that disruption of LRRC8A changes the apparent sizes of the other LRRC8 subunits (prominently seen for LRRC8D in HCT cells) because LRRC8B through E need LRRC8A to leave the ER (Voss *et al*, 2014) and are therefore not fully glycosylated in its absence. *LRRC8D1*$^{-/-}$ and *LRRC8D2*$^{-/-}$ denote two independent HEK and HCT116 knockout clones.

Figure EV2. Increased resistance of *LRRC8A*$^{-/-}$ and *LRRC8D*$^{-/-}$ HAP1 cells to carboplatin and cisplatin, but not to oxaliplatin.

A–C Clonogenic growth of *LRRC8A*$^{-}$ and *LRRC8D*$^{-}$ or WT HAP1 cells treated with carboplatin, cisplatin, or oxaliplatin. Cells were exposed to the indicated concentrations of carboplatin (A), cisplatin (B), or oxaliplatin (C) for 7 days. Surviving colonies were formalin-fixed and stained with crystal violet. The optical absorption was determined at 590 nm after extracting the dye with 10% acetic acid. Data are presented as mean ± SEM (n = 6). CI, confidence interval.

A Carboplatin

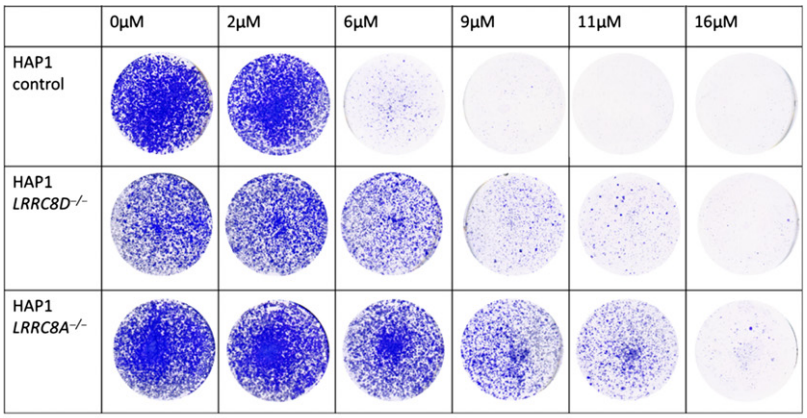

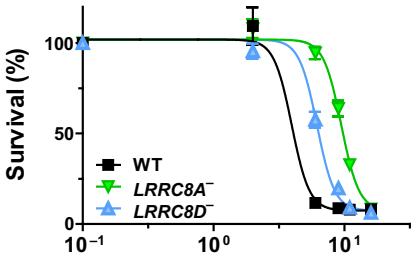

	WT	*LRRC8A*$^{-/-}$	*LRRC8D*$^{-/-}$
IC50 (μM)	4.6	9.1	6.3
CI (95%)	4.1 – 5.1	8.9 – 9.3	6.2 – 6.5

B Cisplatin

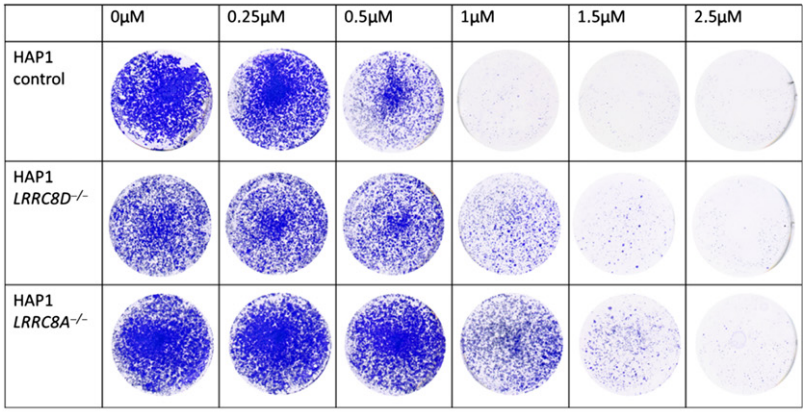

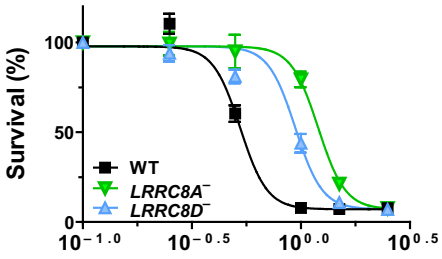

	WT	*LRRC8A*$^{-/-}$	*LRRC8D*$^{-/-}$
IC50 (μM)	0.28	1.20	0.74
CI (95%)	–0.03 – 0.59	1.04 – 1.35	0.63 – 0.85

C Oxaliplatin

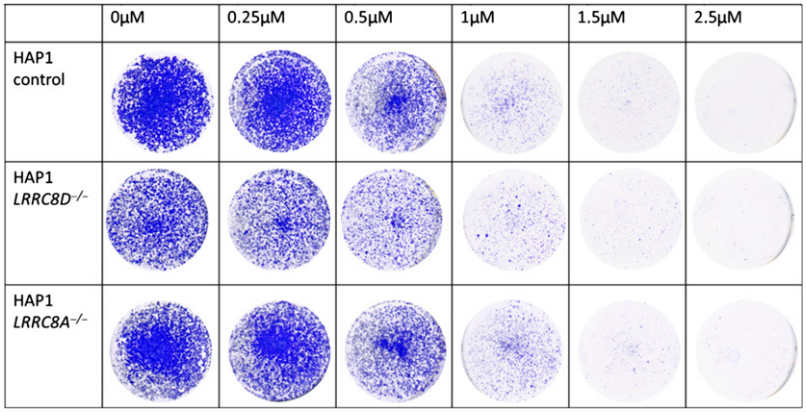

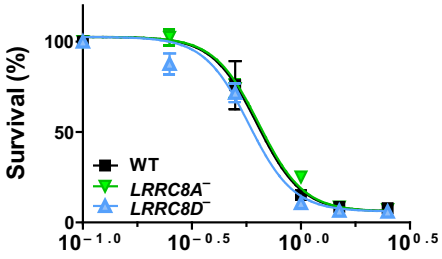

	WT	*LRRC8A*$^{-/-}$	*LRRC8D*$^{-/-}$
IC50 (μM)	0.45	0.50	0.36
CI (95%)	0.16 – 0.75	0.34 – 0.66	0.16 – 0.57

Figure EV2.

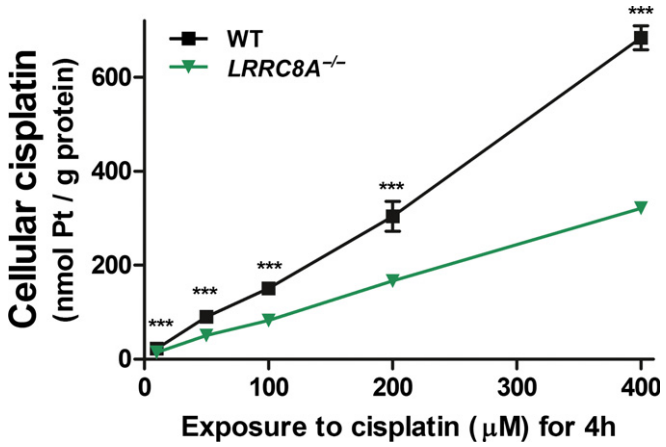

Figure EV3. Pt uptake after 4 h exposure to different concentrations of cisplatin in WT and *LRRC8A*$^{-/-}$ HEK cells.
Cells were exposed to the indicated drug concentrations in isotonic cell culture medium, and accumulated cisplatin was determined by Pt measurements. Data are presented as mean ± SEM (n = 4). ***P < 0.001.

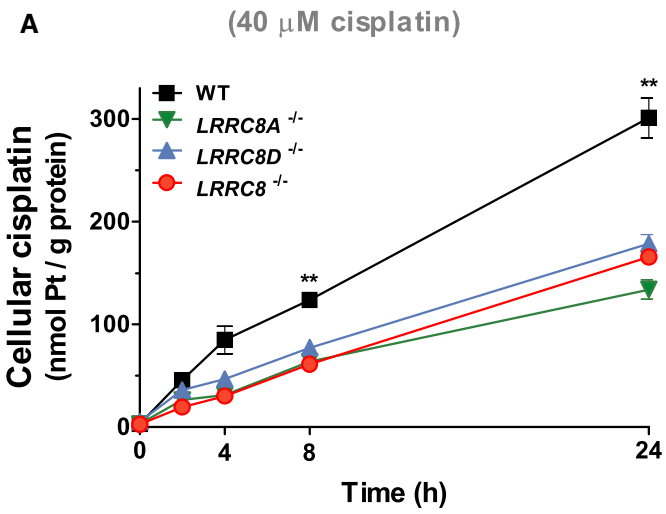

Figure EV4. LRRC8 subunit- and osmolarity-dependent cisplatin uptake in HCT116 cells.
A Long-term cisplatin uptake into WT, *LRRC8A*$^{-/-}$, *LRRC8D*$^{-/-}$, and *LRRC8*$^{-/-}$ HCT116 cells from isotonic culture medium containing 40 μM cisplatin.
B Comparison between short-term uptake from isotonic and hypotonic saline containing 200 μM cisplatin into WT, *LRRC8A*$^{-/-}$, *LRRC8D*$^{-/-}$, and *LRRC8*$^{-/-}$ HCT116 cells.

Data information: Results from two different *LRRC8A*$^{-/-}$ and *LRRC8D*$^{-/-}$ clones each are shown averaged as in Fig 4. Data are presented as mean ± SEM (n = 3). *P < 0.05; and **P < 0.01 compared to *LRRC8A*$^{-/-}$ cells.

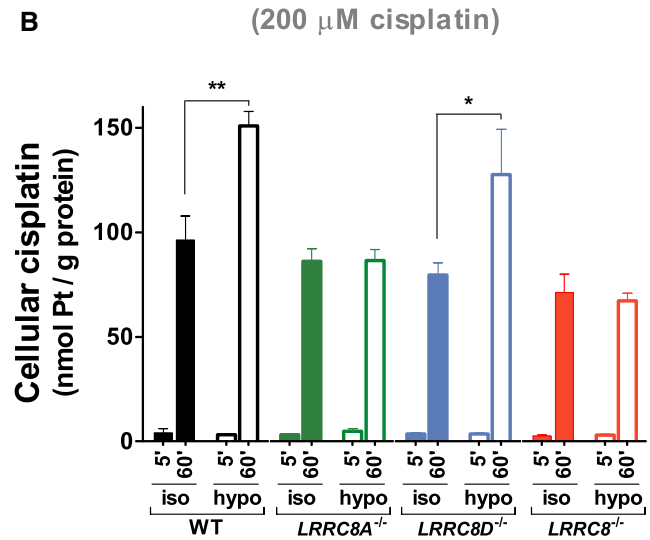

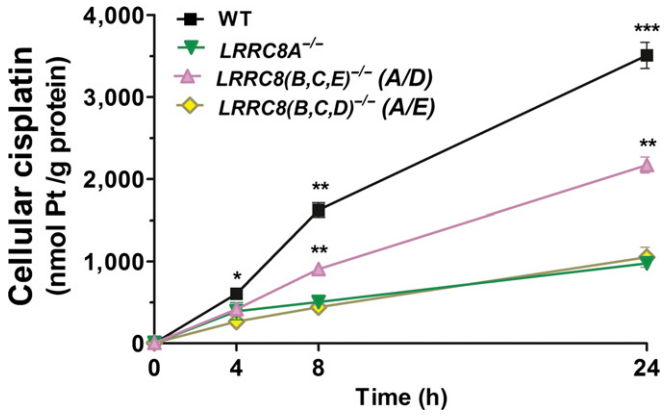

Figure EV5. LRRC8 subunit-dependent uptake of cisplatin into HEK cells of various genotypes.

Cisplatin uptake under isotonic conditions (200 μM cisplatin in culture medium) into HEK WT, *LRRC8A*$^{-/-}$, *LRRC8(B,C,E)*$^{-/-}$ (expressing only A and D subunits), and *LRRC8(B,C,D)*$^{-/-}$ (expressing only A and E) cells during the indicated times. Data are presented as mean ± SEM (n = 3). *P < 0.05; **P < 0.01; and ***P < 0.001 compared to *LRRC8A*$^{-/-}$ cells.

Appendix for

VRAC channel composition influences its substrate specificity and cellular resistance to Pt-based anti-cancer drugs

Rosa Planells-Cases, Darius Lutter, Charlotte Guyader, Nora M. Gerhards, Florian Ullrich, Deborah A. Elger, Asli Kucukosmanoglu, Guotai Xu, Felizia K. Voss, S. Momsen Reincke, Tobias Stauber, Vincent A. Blomen, Daniel J. Vis, Lodewyk F. Wessels, Thijn R. Brummelkamp, Piet Borst, Sven Rottenberg* and Thomas J. Jentsch*

*Corresponding authors. E-mail: Jentsch@fmp-berlin.de (T.J.J.); sven.rottenberg@vetsuisse.unibe.ch (S.R.)

Table of Contents

Appendix to Planells-Cases et al. (2015)

Appendix Figures

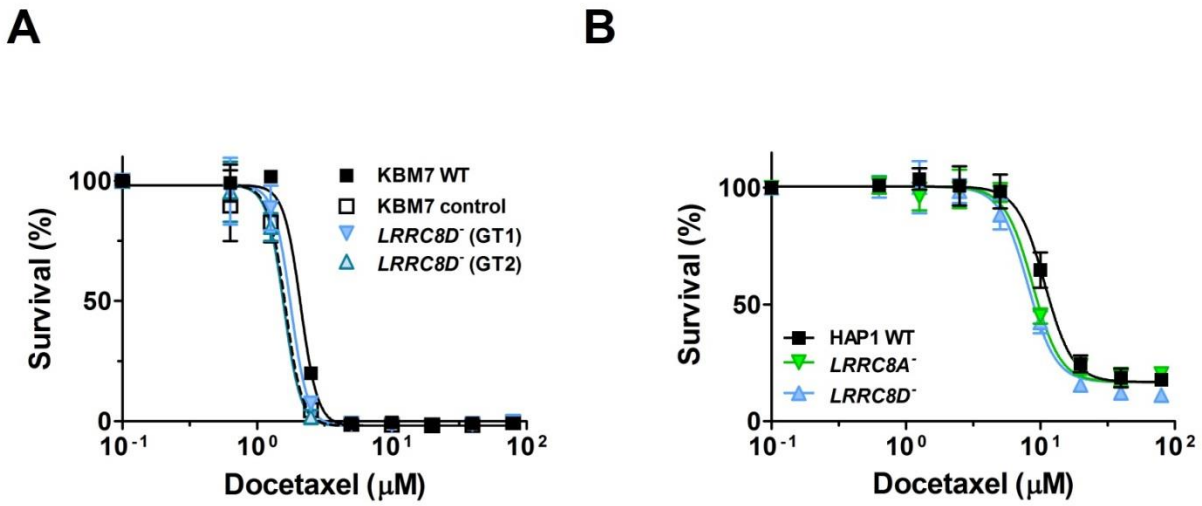

Appendix Figure S1. Docetaxel cytotoxicity assays of *LRRC8D*- or *LRRC8A*-deficient cells.

A. Survival (%) of parental, vector-transduced or *LRRC8D*-deficient GT1 and GT2 KBM7 cells exposed to increasing concentrations of docetaxel.

B. Survival of WT control, *LRRC8A*-, or *LRRC8D*-deficient HAP1 cells. n=3; error bars, standard deviation.

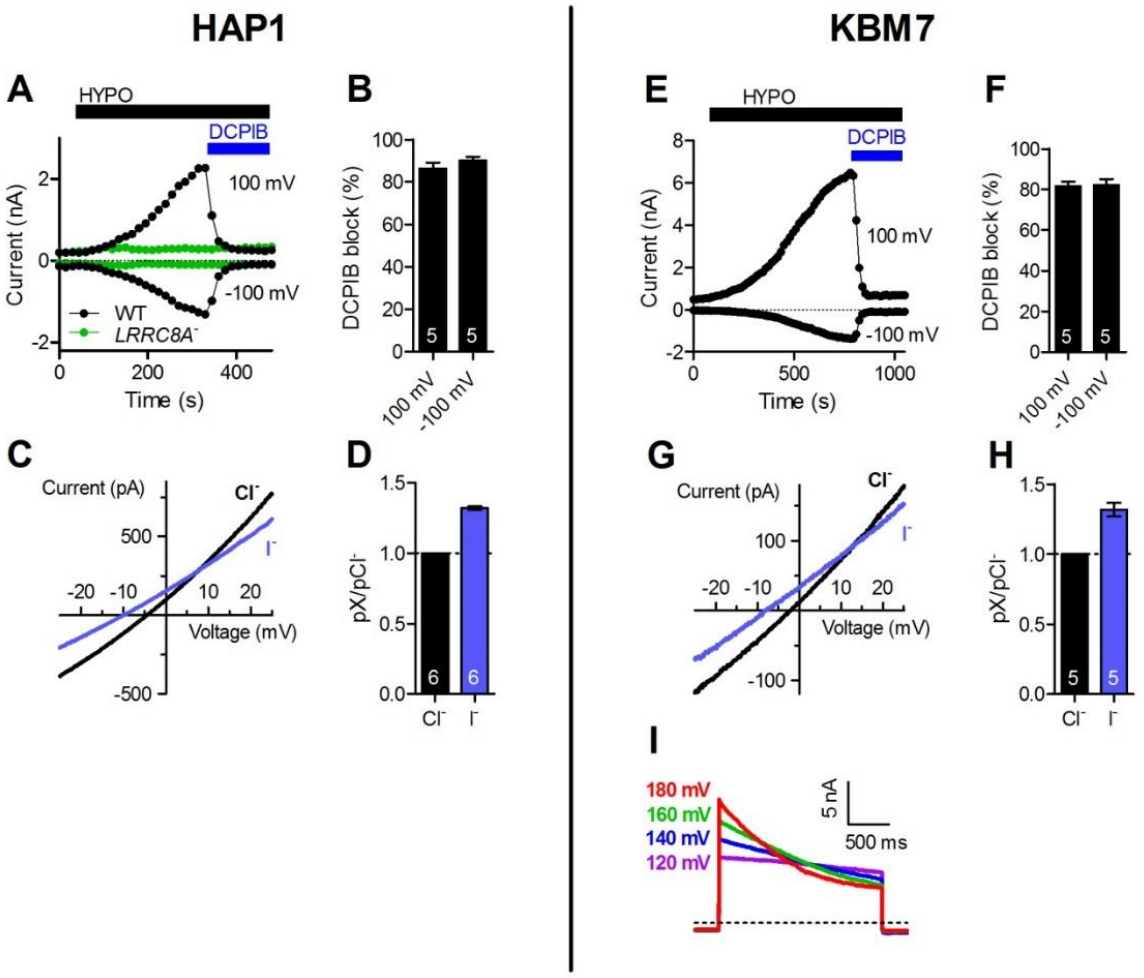

Appendix Figure S2. Characteristics of swelling-induced whole-cell currents recorded from HAP1 and KBM7 cells are consistent with $I_{Cl,vol}$.

A. Example of hypotonicity-activated currents in WT (black) and *LRRC8A*$^-$ (green) HAP1 cells at -100 mV and +100 mV registered every 15 s. Currents depended on LRRC8A and were rapidly inhibited by the VRAC inhibitor DCPIB (20 µM; TOCRIS).

B. Percentage of swelling-activated current in WT HAP1 cells at -100 mV and +100 mV blocked by 20 µM DCPIB.

C. Example current-voltage (I/V) relationships obtained from WT HAP1 cells at the time of maximal current activation with Cl^-- (black) and I^--containing (blue) hypotonic extracellular solutions. When Cl^- is substituted for I^-, the reversal potential shifts to the left, indicating the $I^- > Cl^-$ selectivity typical for $I_{Cl,vol}$.

D. Relative anion permeability (PX/PCl^-) as determined from shifts in reversal potential upon anion substitution (as seen in panel C). Relative permeabilities were calculated as described previously (Voss et al, 2014).

E. Example hypotonicity-activated currents in WT KBM7 cells at -100 mV and +100 mV registered every 15 s. Currents were rapidly inhibited by DCPIB (20 μM).

F. Percentage of swelling-activated current in KBM7 cells at -100 mV and +100 mV blocked by 20 μM DCPIB.

G. Example I/V relationships from WT KBM7 cells at the time of maximal activation with Cl- (black) and I--containing (blue) hypotonic extracellular solutions.

H. Relative anion permeability (PX/PCl^-) as determined from shifts in reversal potential upon anion substitution (as seen in panel G).

I. Example swelling-activated currents from KBM7 cells in response to the indicated voltages, displaying voltage-dependent inactivation at strongly depolarized potentials. The dashed line indicates zero current.

B,D,F,H, the number of cells is indicated on the bars. Error bars, SEM.

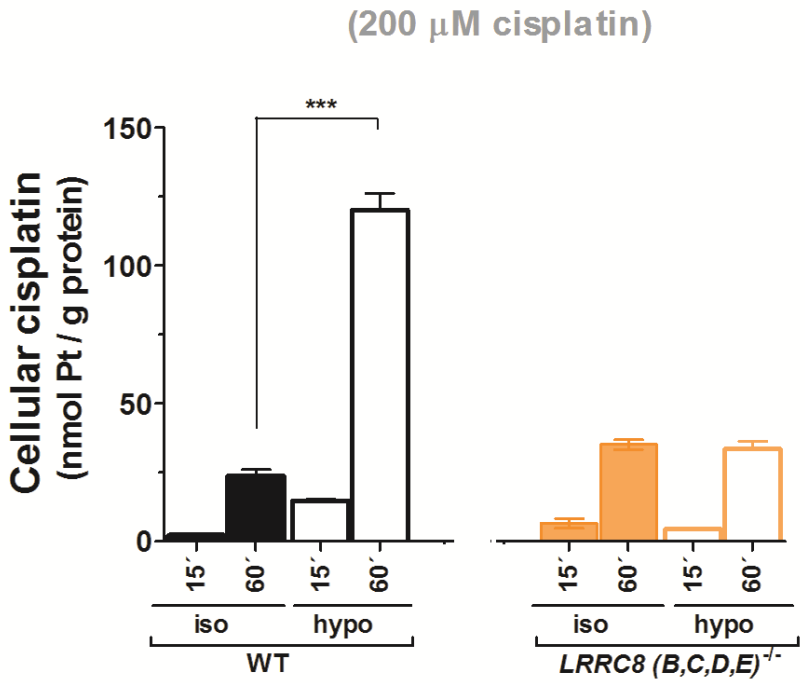

Appendix Figure S3. LRRC8 heteromers are required for cisplatin uptake.

Parallel disruption of LRRC8B-E abolishes swelling-activated cisplatin uptake (200 μM) into HCT116 cells, demonstrating that heteromers of LRRC8A with at least one other LRRC8 isoform are needed for uptake. Similar results were previously obtained for $I_{Cl,vol}$ (*1*). n=3; error bars, SEM. ***, p<0.001.

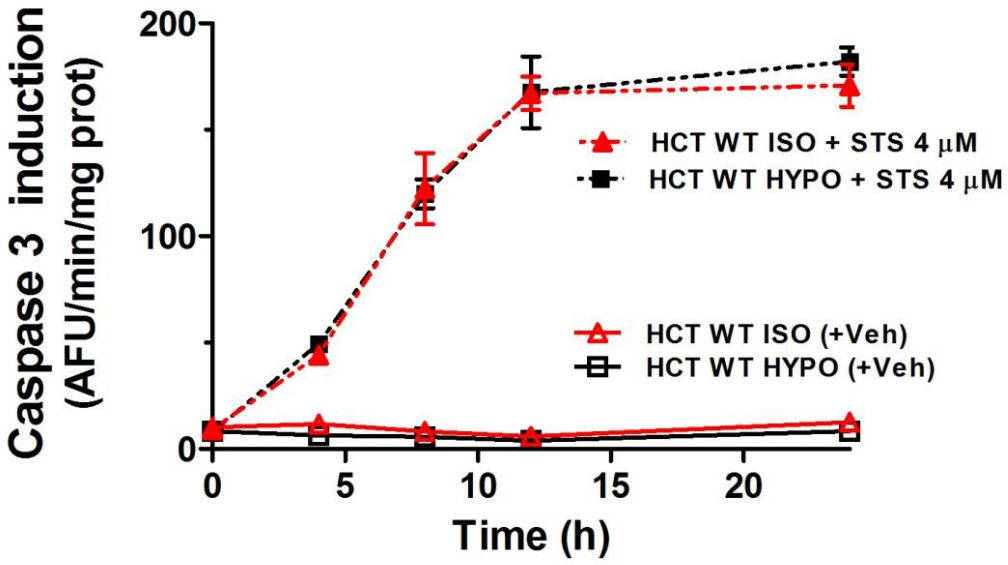

Appendix Figure S4. One-hour exposure to hypotonic solution did not induce caspase activity in HCT116 cells.

Exposure to 4 μM staurosporine for the same time induced caspase 3 irrespective of tonicity. Red and black lines correspond to cells treated for 1 h with isotonic- and hypotonic-saline, respectively (always containing 0.4% DMSO). Dotted lines correspond to cells exposed to staurosporine (STS) while solid lines denote vehicle-treated cells. AFU, arbitrary fluorescence units from enzymatic assay (see Methods). n=3; error bars, SEM.

Gene	Disruptive Insertions in Screen	Total Other Disruptive Insertions in Screen	Disruptive Insertions in Control	Total Other Disruptive Insertions in Control	p value	FDR-adjusted p value
LRRC8D	**49**	**1649**	**104**	**212574**	**8.0E-64**	**1.0E-60**
LRRC8A	**7**	**1691**	**11**	**212667**	**5.7E-11**	**3.6E-8**
MAP4K5	5	1693	17	212661	7.3E-07	0.0003
SEC24B	3	1695	4	212674	1.7E-05	0.004
SLFN11	4	1694	16	212662	1.7E-05	0.004

Appendix Table S1. Enrichment of gene-trap insertions in the population of KBM7 cells treated with carboplatin (screen) versus the control.

The number of insertion sites per gene and the total number of insertions of the carboplatin selected cells (screen) was compared to an unselected mutagenized population (control) as described previously (Carette et al, 2011). A one-sided Fisher exact test was used to calculate the p value. Correction for multiple testing for p values was carried out using the Benjamini and Hochberg FDR-correction.

	KBM7	KBM7 vector	*LRRC8D*^{GT1}	*LRRC8D*^{GT2}
Carboplatin				
IC50 (μM)	3.7	3.4	12.6	11.3
CI (95%)	2.5 - 5.5	2.1 - 5.5	7.3 - 22.0	6.3 - 20.3
Cisplatin				
IC50 (μM)	0.16	0.18	0.74	0.73
CI (95%)	0.10 - 0.26	0.11 - 0.29	0.48 - 1.144	0.43 - 1.22
Oxaliplatin				
IC50 (μM)	2.2	2.5	2.6	1.9
CI (95%)	1.2 – 3.7	1.6 – 4.0	1.7 – 3.7	1.3 – 2.7

Appendix Table S2. IC50 (average) and 95% confidence interval (CI) of the data presented in Fig. 1 for cisplatin, carboplatin and oxaliplatin.

Results were obtained from three independent experiments.

References

Carette JE, Guimarães CP, Wuethrich I, Blomen VA, Varadarajan M, Sun C, Bell G, Yuan B, Muellner MK, Nijman SM, Ploegh HL, Brummelkamp TR (2011) Global gene disruption in human cells to assign genes to phenotypes by deep sequencing. Nature biotechnology 29: 542-546

Voss FK, Ullrich F, Münch J, Lazarow K, Lutter D, Mah N, Andrade-Navarro MA, von Kries JP, Stauber T, Jentsch TJ (2014) Identification of LRRC8 heteromers as an essential component of the volume-regulated anion channel VRAC. Science 344: 634-638